BIOCHEMISTRY

Nicotinamide riboside and nicotinamide mononucleotide facilitate NAD^+ synthesis via enterohepatic circulation

Keisuke Yaku[1]†, Sailesh Palikhe[1]†‡, Tooba Iqbal[1], Faisal Hayat[2], Yoshiyuki Watanabe[3], Shiho Fujisaka[3], Hironori Izumi[4,5], Tomoyuki Yoshida[4,5], Mariam Karim[1], Hitoshi Uchida[1], Allah Nawaz[1], Kazuyuki Tobe[3,6], Hisashi Mori[4,5], Marie E. Migaud[2], Takashi Nakagawa[1,6]*

Decreased nicotinamide adenine dinucleotide (oxidized form) (NAD^+) levels are reportedly associated with several aging-related disorders. Thus, supplementation with NAD^+ precursors, such as nicotinamide mononucleotide (NMN) and nicotinamide riboside (NR), exhibits beneficial effects against these disorders. However, the in vivo metabolic pathways of NMN and NR remain to be elucidated. In this study, we comprehensively analyzed the fate of orally and intravenously administered NMN and NR in mice using NAD^+ metabolomics. We found that only a small portion of orally administered NMN and NR was directly absorbed from the small intestine and that most of them underwent gut microbiota–mediated deamidation and conversion to nicotinic acid (NA). Moreover, intravenously administered NMN and NR were rapidly degraded into nicotinamide and secreted to bile followed by deamidation to NA by gut microbiota. Thus, enterohepatic circulated NA is preferentially used in the liver. These findings showed that NMN and NR are indirectly converted to NAD^+ via unexpected metabolic pathways.

INTRODUCTION

Nicotinamide adenine dinucleotide (oxidized form) (NAD^+) is a versatile molecule that is associated with redox reactions, protein posttranslational modification, molecular signaling, and mRNA stability (*1*). Pathological burden and aging decrease NAD^+ levels in cells and tissues by changing the balance between NAD^+ synthesis and degradation, resulting in the deterioration of physiological functions (*2*, *3*). Thus, boosting or restoring NAD^+ levels exhibits benefits against physiological aging and its associated disorders, including obesity, muscle degeneration, and neurodegeneration (*4*–*8*). NAD^+ precursor administration is a simple and convenient strategy to activate NAD^+ synthesis and increase NAD^+ levels (*9*). Recently, nicotinamide riboside (NR) and nicotinamide mononucleotide (NMN) have attracted increasing interest as alternative NAD^+ precursors (*4*, *9*). NMN is an intermediate in the salvage pathway and can be converted to NAD^+, bypassing a catalysis of nicotinamide phosphoribosyltransferase (NAMPT), a rate-limiting enzyme in this pathway (*10*). Meanwhile, NR is converted to NMN by NR kinase (NRK), thereby bypassing the NAMPT-mediated step (*11*, *12*). Therefore, NMN and NR are thought to efficiently increase NAD^+ levels compared with classical NAD^+ precursors, such as nicotinamide (NAM) and nicotinic acid (NA). Accordingly, preclinical and clinical studies have demonstrated that NMN and NR administration provides beneficial effects, especially against metabolic dysfunctions and age-associated diseases, including obesity, insulin resistance, neurodegenerative diseases, and age-related decline in fertility (*13*–*19*). However, NR and NMN supplementation exhibited minimal or no efficacy against aging and age-associated diseases in several clinical trials, suggesting that further investigation of NAD^+ metabolism is necessary (*20*, *21*).

In humans and rodents, NAD^+ precursors are usually given through oral administration (*1*). Recent studies indicated that the gut microbiota is essentially involved in the host NAD^+ metabolism network (*22*–*24*). Most bacteria have a NAM deamidase, an enzyme that converts NAM into NA. However, mammals do not have a homologous enzyme (*12*, *25*–*28*). The conversion of NAM into NA by gut microbiota is important for the oral administration of NAD^+ precursors that can be converted to NAD^+. For example, the gut microbiota deamidates orally administered NAM to NA, which is then used for NAD^+ synthesis via the Preiss-Handler pathway in the liver (*23*). Recently, we have shown that orally administered NR increases hepatic NAD^+ levels in a diphasic manner (*22*). In the early phase (approximately 30 min after oral administration), the direct absorption of NR from the small intestine contributed to NAD^+ synthesis. However, excess NR was not completely absorbed from the small intestine, but instead were hydrolyzed to NAM by bone marrow stromal cell antigen 1, which is dominantly expressed on the luminal surface of the epithelium in the small intestine. As NR-derived NAM reached the large intestine, the gut microbiota deamidated NAM into NA. Subsequently, NA was absorbed from the large intestine and contributed to NAD^+ synthesis in the liver through the Preiss-Handler pathway in the late phase (approximately 3 hours after oral administration). NMN is a substrate for nicotinamide mononucleotide adenylyltransferase (NMNAT), which is an enzyme that converts NMN and adenosine triphosphate to NAD^+ and inorganic pyrophosphate (*10*). However, several studies have suggested that NMN is not directly absorbed by cells but is extracellularly converted

[1]Department of Molecular and Medical Pharmacology, Faculty of Medicine, University of Toyama, 2630 Sugitani, Toyama, Toyama 930-0194, Japan. [2]Mitchell Cancer Institute, Department of Pharmacology, University of South Alabama, 1660 Springhill Avenue, Mobile, AL 36693, USA. [3]First Department of Internal Medicine, Faculty of Medicine, University of Toyama, 2630 Sugitani, Toyama, Toyama 930-0194, Japan. [4]Department of Molecular Neuroscience, Faculty of Medicine, University of Toyama, 2630 Sugitani, Toyama, Toyama 930-0194, Japan. [5]Research Center for Idling Brain Science (RCIBS), University of Toyama, 2630 Sugitani, Toyama, Toyama 930-0194, Japan. [6]Research Center for Pre-Disease Science, University of Toyama, 2630 Sugitani, Toyama, Toyama 930-0194, Japan.
*Corresponding author. Email: nakagawa@med.u-toyama.ac.jp
†These authors contributed equally to this work.
‡Present address: Department of Cell Biology and Physiology, University of Kansas Medical Center, Kansas City, KS, USA.

to NR by CD73, also known as 5′-nucleotidase ecto (NT5E), and then absorbed as the form of NR (*29*–*31*). In a previous study, the deficiency of NRK1, which phosphorylates NR to NMN, diminished the increase of NAD^+ levels in the liver after oral NMN administration, suggesting that NMN was converted to NR before absorption (*11*). By contrast, another study found that Slc12a8 was an NMN transporter and demonstrated that NMN was directly absorbed from the small intestine and contributed to NAD^+ synthesis (*32*). Moreover, a recent study found that orally administered NMN was converted to nicotinic acid mononucleotide (NAMN) through deamidation by the gut microbiota (*33*). The gut microbiota also influenced host NAD^+ metabolism by deamidating NAM coming across the blood vessels (*24*). Intravenously injected NAM cycled between the host tissue and the gut microbiome. However, the route of this cycle remains unclear. Therefore, further studies are needed to clarify the metabolic pathway of orally administered NMN to improve in vivo NMN availability.

In the present study, we comprehensively analyzed the fate of orally and intravenously administered NMN and NR in mice using NAD^+ metabolomics. We found that only a small portion of orally administered NMN and NR was directly absorbed from the small intestine and that most of them underwent conversion to NAM and NA in the gut lumen. NMN-derived NA was preferentially used to synthesize NAD^+ in the liver via the Preiss-Handler pathway. Moreover, we observed that bile circulation and gut microbiota were required to boost NAD^+ synthesis in the liver when NR and NMN were intravenously administered. These findings showed that most of NMN and NR do not directly contribute to NAD^+ synthesis. Instead, they undergo degradation to NAM and deamidation to NA, which is then used for NAD^+ synthesis.

RESULTS

Gavaged NMN and NR were directly absorbed from the small intestine

To reveal the metabolic pathway of orally NMN and NR, we performed a time course NAD^+ metabolome analysis after a single oral gavage of NMN as well as NR. Oral gavage of NMN significantly increased NMN levels in the small intestine at 15 min (Fig. 1B). Moreover, the rise of NMN by oral gavage of NR was much lower (approximately 25-fold less) than that by oral gavage of NMN (Fig. 1B). These results demonstrated that a certain amount of NMN is directly taken up by the small intestine during oral administration. In addition, the increase of NR levels by NMN administration was slightly delayed compared with that by NR administration (Fig. 1B). The increase of NR levels in the small intestine after oral gavage of NMN indicated that NMN is rapidly dephosphorylated to become NR. We also measured deamidated NAD^+ metabolome, including nicotinic acid adenine dinucleotide (NAAD) and NAMN. We found that NAAD and NAMN were significantly increased in the small intestine at later time points (180 and 360 min) (Fig. 1B). However, NAD^+ levels in the small intestine peaked at 15 to 30 min after the administration of NMN and NR, respectively (Fig. 1B). These results suggested that NAD^+ synthesis in the small intestine is mainly from directly absorbed NMN and NR via the salvage pathway.

We also confirmed the direct uptake of NR and NMN using cultured cells. NMN treatment to A549 cells increased NMN levels at 1 min, which were maintained until 4 hours (Fig. 1C). Similarly, NR treatment increased NR levels at 1 min (Fig. 1C). Meanwhile, NMN treatment also increased NR and NAD^+ levels at later time points (Fig. 1C). The earlier rapid increase of NMN levels than NR levels suggested that NMN is directly taken up by A549 cells. CD73 is considered an ectoenzyme responsible for the extracellular conversion of NMN to NR (*31*). Thus, we investigated whether CD73 was required to increase intracellular NAD^+ levels from exogenously supplied NMN. CD73 knockdown in A549 cells using RNAi increased intracellular NAD^+ levels at 4 hours after NMN treatment more than control (Fig. 1D and fig. S1). Moreover, NMN treatment increased intracellular NMN levels in control and knockdown cells but decreased NR levels in knockdown cells (Fig. 1D). These results suggested that some amount of NMN was extracellularly converted to NR by CD73. However, the majority of NMN was directly taken up independent of CD73 and converted to NAD^+ in A549 cells.

Gavaged NMN and NR increased NAD^+ and deamidated metabolite levels

We examined the time course of the NAD^+ metabolome in the liver when NMN and NR were administered to wild-type (WT) mice by single oral gavage. Consistent with our previous results (*22*). the oral administration of NR gradually increased NAD^+ levels with a significant increase of deamidated metabolites, including NAAD, NAMN, and nicotinic acid riboside (NAR), at the late phase (3 to 6 hours) (Fig. 2A). Similar to NR, orally administered NMN gradually increased NAD^+ levels (Fig. 2A). NMN and NAM levels remarkably increased at 3 hours with the significant increase of NAD^+ and deamidated NAD^+ precursors. These results implied that NMN was possibly converted to NAD^+ via the Preiss-Handler pathway in the late phase as well as NR. In addition, we analyzed the NAD^+ metabolome in the large intestine. Similar to the liver, orally administered NMN increased the levels of deamidated metabolites in the large intestine at the late phase (fig. S2A). The increase of NAD^+ peaked at 3 hours and started to decrease at 6 hours, corresponding to the kinetics of deamidated metabolites. In addition, we examined NA levels in the luminal content of the large intestine and found that orally administered NMN generated NA in the colon lumen (fig. S2B). These data suggested that the oral administration of NMN and NR increased the levels of deamidated metabolites in the liver and large intestine, thereby contributing to NAD^+ synthesis in these tissues.

Gut microbiota and the Preiss-Handler pathway are involved in NAD^+ synthesis from NMN

Several studies have demonstrated that the gut microbiota is required to generate deamidated NAD^+ metabolites (e.g., NA, NAR, NAMN, and NAAD) in the liver at the late phase by NR oral administration (*22*–*24*, *33*). We found that the oral administration of NMN also increased the levels of deamidated metabolites in the liver and large intestine (Fig. 2A and fig. S2A). Thus, we considered that the gut microbiota is involved in the generation of deamidated NAD^+ metabolites by the oral administration of NMN. Hence, we administered NMN and NR to germ-free (GF) mice through oral gavage and examined the NAD^+ metabolome in the liver. Consistent with previous results, NR administration did not increase the levels of deamidated metabolites (e.g., NA, NAR, and NAAD) in the liver of GF mice at 3 hours (Fig. 2B). Similarly, the oral administration of NMN completely failed to increase the levels of deamidated metabolites in the liver of GF mice (Fig. 2B). In addition, the increase of NAD^+ levels was significantly suppressed in NMN-administered and NR-administered

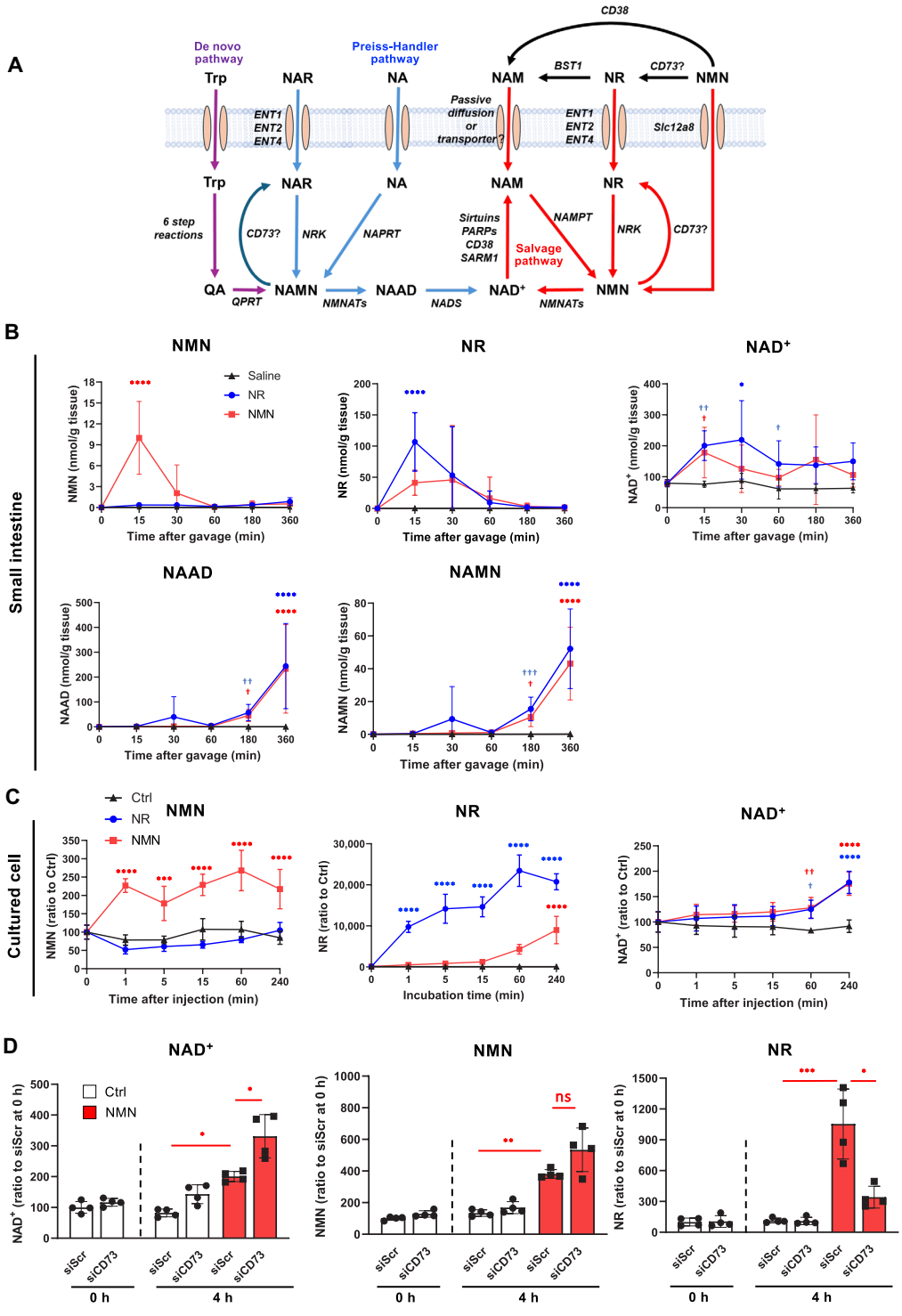

Fig. 1. Orally administered NMN and NR were directly taken up from the small intestine. (**A**) Overview of NAD^+ biosynthesis pathways in mammals. (**B**) Time course analysis of NAD^+ metabolome in the small intestine of WT mice gavaged with NMN and NR. $n = 6$ mice per group. P values of interaction effect; NMN < 0.0001, NR = 0.0022, NAD^+ = 0.2128, NAAD < 0.0001, and NAMN < 0.0001. Statistical significance was determined by Tukey's test. Asterisks (*$P < 0.05$ and ****$P < 0.0001$) indicate significance compared with the saline group at the same time point in the overall analysis. Daggers ($^{\dagger}P < 0.05$, $^{\dagger\dagger}P < 0.01$, and $^{\dagger\dagger\dagger}P < 0.001$) indicate significance compared with the saline group at the same time point in the specific time point analysis. (**C**) Time course analysis of NAD^+ metabolome in A549 cells treated with NMN and NR. $n = 3$ to 4. P values of interaction effect; NMN < 0.0001, NR < 0.0001, and NAD^+ = 0.0032. Statistical significance was determined by Tukey's test. Asterisks (***$P < 0.001$ and ****$P < 0.0001$) indicate significance compared with the saline group at the same time point in the overall analysis. Daggers ($^{\dagger}P < 0.05$ and $^{\dagger\dagger}P < 0.01$) indicate significance compared with the saline group at the same time point in the specific time point analysis. (**D**) Effect of CD73 knockdown on NAD^+ metabolome in A549 cells treated with NMN. $n = 4$. Statistical significance was determined by Tukey's test (*$P < 0.05$, **$P < 0.01$, and ***$P < 0.001$). h, hours.

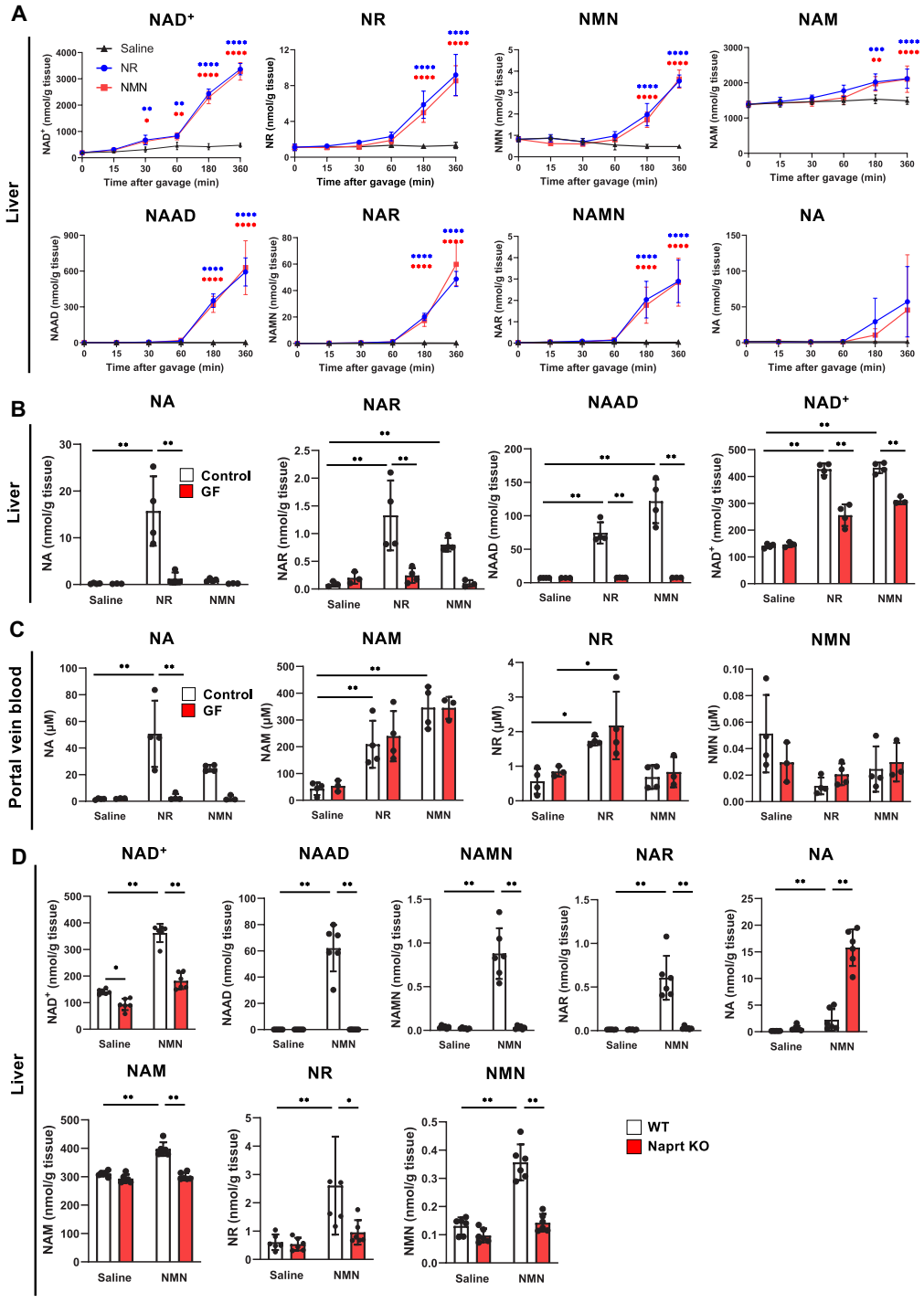

Fig. 2. Gut microbiota and Preiss-Handler pathway are essential for orally administered NMN to increase NAD$^+$ levels in the liver. (**A**) Time course analysis of NAD$^+$ metabolome in the liver of WT mice gavaged with NMN and NR. $n = 6$ mice per group. P values of interaction effect; NAD$^+$ < 0.0001, NR < 0.0001, NMN < 0.0001, NAM < 0.0001, NAAD < 0.0001, NAR < 0.0001, NAMN < 0.0001, and NA = 0.0777. Statistical significance was determined by Tukey's test. Asterisks (*P < 0.05, **P < 0.01, ***P < 0.001, and ****P < 0.0001) indicate significance compared with the saline group at the same time point in the overall analysis. (**B**) NAD$^+$ metabolome in the liver of control and germ-free mice at 3 hours after the oral administration of NMN and NR. $n = 3$ to 4 mice per group. P values of interaction effect; NA = 0.0007, NAR = 0.0069, NAAD < 0.0001, and NAD$^+$ < 0.0001. Statistical significance was determined by Tukey's test (**P < 0.01). (**C**) NAD$^+$ metabolome in the blood from the portal vein of control and germ-free mice at 3 hours after the oral administration of NMN and NR. $n = 4$ mice per group. P values of interaction effect; NA = 0.0024, NAM = 0.9063, NR = 0.8483, and NMN = 0.2144. Statistical significance was determined by Tukey's test (*P < 0.05 and **P < 0.01). (**D**) NAD$^+$ metabolome in the liver of WT and *Naprt* KO mice at 3 hours after the oral administration of NMN and NR. $n = 6$ mice per group. P values of interaction effect; NAD$^+$ < 0.0001, NAAD < 0.0001, NAMN < 0.0001, NAR < 0.0001, NA < 0.0001, NAM < 0.0001, NR = 0.0448, and NMN < 0.0001. Statistical significance was determined by Tukey's test (**P < 0.01).

GF mice (Fig. 2B). Furthermore, NA levels were significantly reduced in the blood from the portal vein of NR- and NMN-administered GF mice, but NAM, NR, and NMN levels remained unchanged (Fig. 2C). These results suggested that microbiota generated NA in the large intestine, thereby contributing to NAD^+ synthesis in the liver.

A previous study demonstrated that NMN was deamidated into NAMN by gut microbiota and then converted into NAD^+ by NMNAT and NAD synthetase (*33*). However, our results implied that gut microbiota generated NA from orally administered NMN for NAD^+ synthesis. Thus, we determined whether orally administered NMN was converted to NA and generated NAD^+ through the Preiss-Handler pathway in the liver. NMN was orally administered to *Naprt* knockout (KO) mice through gavage, and the NAD^+ metabolome in the liver was examined after 3 hours of administration. Expectedly, the rise of hepatic NAD^+ levels after NMN oral administration was significantly suppressed in *Naprt* KO mice (Fig. 2D). The increase of NAAD, NAMN, and NAR levels was also completely suppressed in NMN-administered *Naprt* KO mice, suggesting that NA was not generated from NAMN. Moreover, NA levels significantly increased in the liver of NMN-administered *Naprt* KO mice (Fig. 2D). The increase of metabolites in the salvage pathway (e.g., NAM, NMN, and NR) was also suppressed, suggesting that NAPRT-dependent NAD^+ synthesis supplied NAM and activated the salvage pathway in the liver (Fig. 2D). These data demonstrated that NMN is mainly converted to NA, not to NAMN, by gut microbiota and generated NAD^+ through the Preiss-Handler pathway.

Tracing of stable isotope–labeled NMN and NR for NAD^+ synthesis in the liver

The static snapshot of the NAD^+-related metabolome using GF mice and *Naprt* KO mice revealed the pathways of orally administered NMN and NR. However, these methods interrupted the normal metabolic flow and possibly caused a nonphysiological detouring of pathways. Thus, we used stable isotope–labeled NMN and NR for the kinetic tracing of the NAD^+ metabolome to reveal the natural fate of these NAD^+ precursors. We synthesized stable isotope–labeled [m + 6] NR and [m + 8] NMN and measured various NAD^+ metabolome in the liver at 3 hours after the oral gavage. We orally administered [m + 6] NR and observed a marginal increase of [m + 6]–labeled NAD^+, NMN, and NR levels in the liver, confirming that the direct conversion of NR to NAD^+ was very scarce (Fig. 3, A and B, and fig. S3). By contrast, most of the increased NAD^+ were labeled as [m + 1], [m + 3], and [m + 4], suggesting that NAD^+ was generated from [m + 1] and [m + 3] NA and also [m + 4] NAM (Fig. 3, A and B, and fig. S3). Accordingly, most of the increased NAAD, NAMN, and NA were also labeled as [m + 1] and [m + 3], suggesting that NR was hydrolyzed to NAM and subsequently converted to NA by the gut microbiota (Fig. 3B and fig. S3). Further, most of the increased NR, NMN, and NAM were labeled as [m + 1] and [m + 4]. These data implied that [m + 1] NAD^+ was hydrolyzed to [m + 1] NAM by NAD^+-consuming enzymes and subsequently converted to NR and NMN via the salvage pathway. We also conducted the tracing experiment using isotope-labeled [m + 8] NMN (Fig. 3, C and D, and fig. S4). Similar to the case of the oral administration of NR, small amounts of [m + 8]–labeled NAD^+, NR, and NMN were detected, whereas a significant increase of [m + 1] and [m + 3] NAD^+ was observed in the liver at 3 hours after the oral gavage of NMN (Fig. 3D). Furthermore, the levels of [m + 1] and [m + 3] NAAD, NAMN, and NA were significantly increased (Fig. 3D and fig. S4). In addition, the increased NMN, NR, and NAM were labeled as [m + 1] and [m + 3] (Fig. 3D and fig. S4). These data strengthened our thought that the majority of orally administered NR and NMN were degraded to NA and converted to NAD^+ via the Preiss-Handler pathway in the liver.

Gavaged NMN and NR could not directly increase NAD^+ levels in the skeletal muscle

After passing the liver, orally administered NAD^+ precursors are further distributed to the peripheral organs. The skeletal muscle is considered an important target organ for NAD^+ replenishment therapy (*34*–*36*). Previous studies have shown that the salvage pathway is the main route for NAD^+ synthesis in the skeletal muscle (*35*, *37*, *38*). However, the increase of NAD^+ levels in the skeletal muscle after NR and NMN administration is not as efficient as that in the liver (*17*, *18*, *20*, *39*–*42*). In addition, our data above demonstrated that most of the orally administered NR and NMN were metabolized to NAM and NA before reaching the liver. Thus, we aimed to determine the NAD^+ synthesis pathway in the skeletal muscle when NR and NMN were orally administered. We performed time course NAD^+ metabolome analysis to reveal the fate of orally administered NAD^+ precursors in the skeletal muscle. We found that NAD^+ levels slightly increased at 60 min after the administration of NR or NMN; however, the levels were much lower than those observed in the liver (Fig. 4A). We also found that NR levels were increased 15 min after its administration, while NMN gavage increased its levels at the same time point (Fig. 4A). However, the increase of NMN and NR levels by these precursors returned to baseline at 60 min (Fig. 4A). By contrast, NAM levels gradually increased and were sustained at the late phase after NR and NMN administration (Fig. 4A). The levels of deamidated NAD^+ precursors, including NAAD, NAR, NAMN, and NA, were also increased at the late phase. However, the levels of these precursors in the skeletal muscle were much lower than those in the liver (e.g., NAAD was 100-fold lower when compared to the results in Fig. 2A), suggesting that deamidated precursors were not the main source for NAD^+ synthesis (Fig. 4A). To examine this, we performed tracing experiments using [m + 6] NR and [m + 8] NMN (Fig. 4, B and C, and figs. S5 and S6). Labeled NR was orally administered to WT mice, and the skeletal muscle of WT mice was harvested at 3 hours after administration (Fig. 4B and fig. S5). Although [m + 6] NR was significantly increased, the increase of [m + 6] NAD^+ was extremely low, suggesting that NAD^+ was not directly generated from NR (Figs. 3A and 4B and fig. S5). On the other hand, [m + 0], [m + 1], and [m + 4] NAD^+ significantly increased. We also found that [m + 1] and [m + 4] NAM were significantly increased (Fig. 4B and fig. S5). These data suggested that orally administered NR did not directly contribute to NAD^+ synthesis, whereas NAM hydrolyzed from administered NR could be a source for NAD^+ synthesis in the skeletal muscle. In addition, [m + 1] NAM, which may be generated in the liver via the Preiss-Handler pathway and subsequent NAD^+ hydrolysis, could be used for [m + 1] NAD^+ synthesis in the skeletal muscle. However, we could not exclude the possibility that [m + 1] NA was used to generate [m + 1] NAD^+ via the Preiss-Handler pathway in the skeletal muscle. [m + 1] NAAD, NAMN, and NA were significantly increased although the absolute amount was much lower than those in the liver (Figs. 3B and 4B).

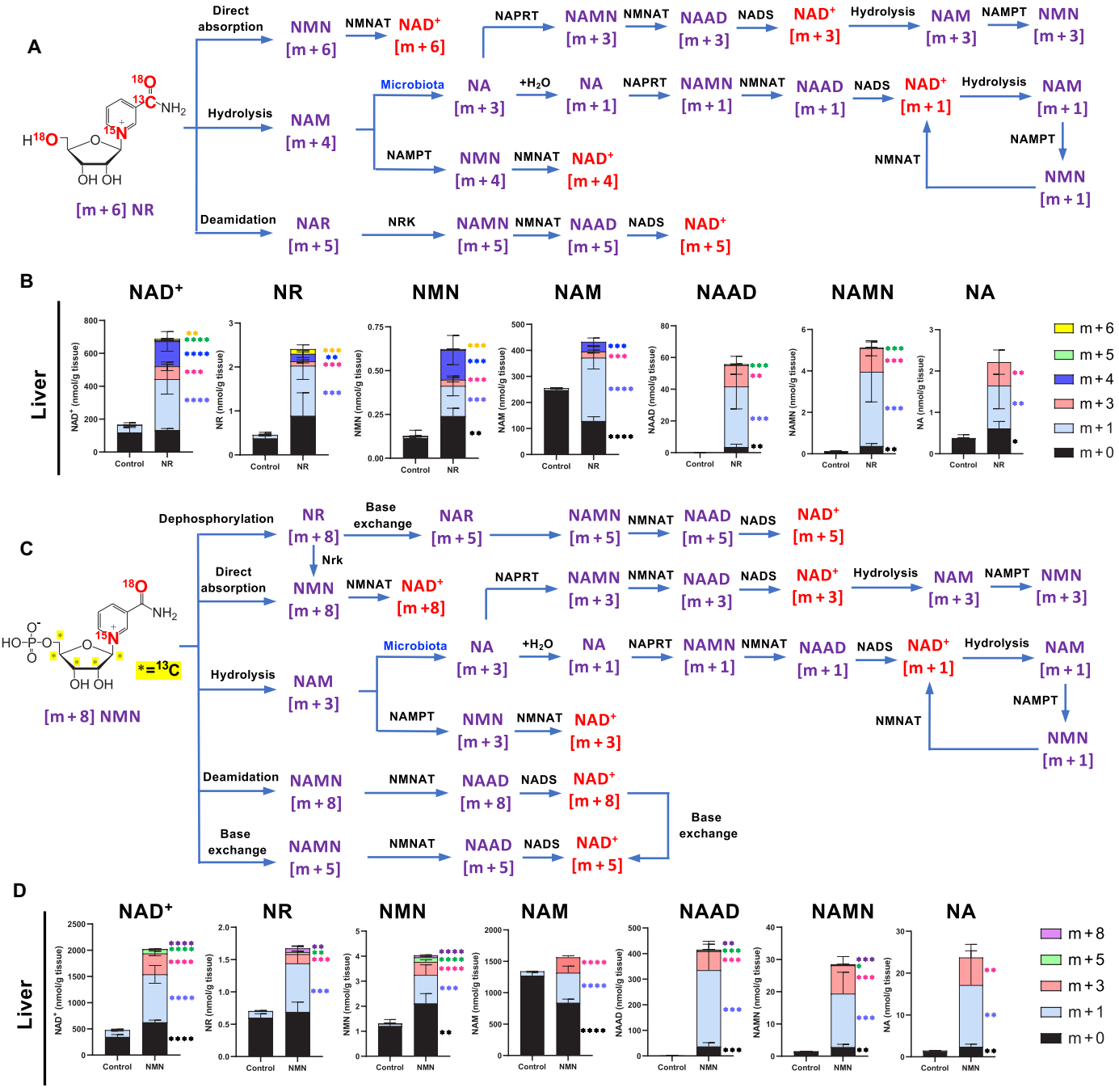

Fig. 3. Tracing of orally administered stable isotope–labeled NMN and NR revealed that NAD$^+$ synthesis through gut microbiota and Preiss-Handler pathway was the major route in the liver. (**A**) Scheme of formation of stable isotope–labeled NAD$^+$ metabolites after the oral administration of [m + 6] NR. (**B**) NAD$^+$ metabolome in the liver of WT mice at 3 hours after the oral administration of [m + 6] NR. $n = 5$ mice for saline group and $n = 4$ mice for NR-treated group. Statistical significance was determined by Student's t test (*$P < 0.05$, **$P < 0.01$, ***$P < 0.001$, and ****$P < 0.0001$). (**C**) Scheme of formation of stable isotope–labeled NAD$^+$ metabolites after the oral administration of [m + 8] NMN. (**D**) NAD$^+$ metabolome in the liver of WT mice at 3 hours after the oral administration of [m + 8] NMN. $n = 5$ mice for saline group and $n = 4$ mice for NMN-treated group. Statistical significance was determined by Student's t test (*$P < 0.05$, **$P < 0.01$, ***$P < 0.001$, and ****$P < 0.0001$).

Next, we examined the NAD$^+$ metabolome in the skeletal muscle when [m + 8] NMN was orally administered (Fig. 4C and fig. S6). Although the administration of [m + 8] NMN increased the total pool of NMN, the majority of them were [m + 0]–, [m + 1]–, and [m + 3]–labeled forms, suggesting that the administered NMN did not directly reach the skeletal muscle (Figs. 3C and 4C and fig. S6). Accordingly, the majority of increased NAD$^+$ were [m + 1]– and [m + 3]–labeled forms (Fig. 4C and fig. S6). We also found that the increased NAM were mainly [m + 1]– and [m + 3]–labeled forms (Fig. 4C and fig. S6). These data suggested that the source of NAD$^+$ in the skeletal muscle was also not NMN but NAM when NMN was orally administered. However, the increased deamidated metabolites,

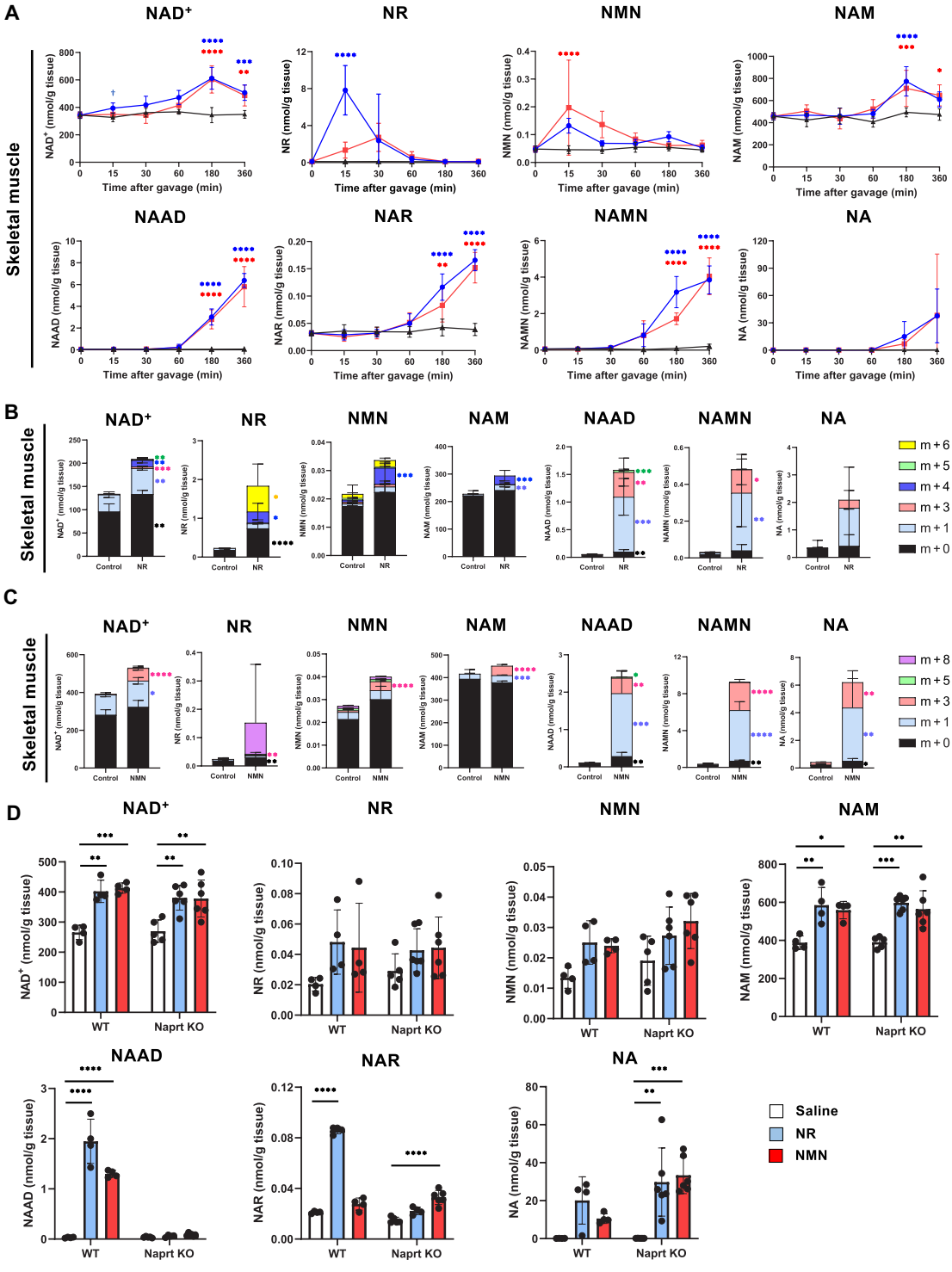

Fig. 4. NAM cleaved from orally administered NR and NMN was preferentially used for NAD^+ synthesis in the skeletal muscle. (**A**) Time course analysis of muscle NAD^+ metabolome in mice gavaged with NMN and NR. $n = 6$ mice per group. P values of interaction effect; $NAD^+ < 0.0001$, NR < 0.0001, NMN = 0.0020, NAM = 0.0002, NAAD < 0.0001, NAR < 0.0001, NAMN < 0.0001, and NA = 0.1543. Statistical significance was determined by Tukey's test. Asterisks (*$P < 0.05$, **$P < 0.01$, ***$P < 0.001$, and ****$P < 0.0001$) indicate significance versus the saline group at the same time point in the overall analysis, while daggers ($^{\dagger}P < 0.05$) indicate significance in the specific time point analysis. (**B**) Muscle NAD^+ metabolome in mice at 3 hours after the oral administration of [m + 6] NR. $n = 5$ (saline group) and $n = 4$ (NR group). Statistical significance was determined by Student's t test (*$P < 0.05$, **$P < 0.01$, ***$P < 0.001$, and ****$P < 0.0001$). (**C**) Muscle NAD^+ metabolome in mice at 3 hours after the oral administration of [m + 8] NMN. $n = 5$ (saline group) and $n = 4$ (NMN group). Statistical significance was determined by Student's t test (*$P < 0.05$, **$P < 0.01$, ***$P < 0.001$, and ****$P < 0.0001$). (**D**) Muscle NAD^+ metabolome in WT and *Naprt* KO mice at 3 hours after the oral administration of NMN and NR. $n = 4$ to 6 mice per group. P values of interaction effect; $NAD^+ = 0.5991$, NR = 0.7034, NMN = 0.6969, NAM = 0.9819, NAAD < 0.0001, NAR < 0.0001, and NA = 0.0885. Statistical significance was determined by Tukey's test (*$P < 0.05$, **$P < 0.01$, ***$P < 0.001$, and ****$P < 0.0001$).

including NAAD, NAMN, and NA, were mainly [m + 1]– and [m + 3]–labeled forms (Fig. 4C and fig. S6). Similar to NR administration, it is still possible that the generation of [m + 1] and [m + 3] NAD^+ was from [m + 1] and [m + 3] NA via the Preiss-Handler pathway in the skeletal muscle.

To determine whether the skeletal muscle can generate NAD^+ from NA via the Preiss-Handler pathway, we administered NR and NMN to *Naprt* KO mice and measured the NAD^+ metabolome in the skeletal muscle at 3 hours. Expectedly, the increase of deamidated NAD^+ precursors by NR and NMN administration was completely suppressed in the skeletal muscle of *Naprt* KO mice (Fig. 4D). However, NR and NMN administration could increase NAD^+ levels as well as NAM levels in *Naprt* KO mice, suggesting that the increase of NAD^+ levels in the skeletal muscle was not generated via the Preiss-Handler pathway, but the salvage pathway using NAM.

NAD^+ synthesis during repeated NMN and NR oral administration in the liver

As single-dose oral administration of NMN failed to increase NAD^+ levels in the liver of *Naprt* KO mice, we aimed to determine the role of the Preiss-Handler pathway during repeated oral administration. Therefore, we administered NMN and NR to WT and *Naprt* KO mice through oral gavage for 2 weeks. Similar to single-dose administration, the repeated oral administration of NMN and NR significantly increased NAD^+ levels in the liver of WT mice but not those of *Naprt* KO mice (fig. S7A). In the skeletal muscle, NAD^+ levels still increased in *Naprt* KO mice after the repeated oral administration of NMN and NR, confirming that NAD^+ synthesis in the skeletal muscle was independent of the Preiss-Handler pathway (fig. S7B). Together, we concluded that NAD^+ synthesis from orally administered NMN and NR in the liver was mainly conducted via the Preiss-Handler pathway and that the contribution of direct conversion from NR and NMN to NAD^+ via the salvage pathway is very marginal during repeated oral administration.

Intravenous injection of NR and NMN also generated deamidated NAD^+ metabolome

Our results demonstrated that orally administered NMN and NR could not be direct precursors for NAD^+ synthesis in the liver and skeletal muscle. Moreover, the increase of NAD^+ levels in the skeletal muscle via oral administration was inefficient compared to that in the liver. Therefore, we wished to examine whether the intravenous injection of these precursors efficiently and directly increased NAD^+ levels in the liver and skeletal muscle. Intravenously injected NR and NMN significantly increased serum NR and NMN levels at 5 min, respectively (Fig. 5A). However, NR and NMN levels in serum rapidly decreased while NAM levels increased, suggesting that NR and NMN were rapidly degraded into NAM in the blood (Fig. 5A). In the liver, intravenously injected NR and NMN efficiently increased NAD^+ levels with a significant increase of NR, NMN, and NAM at 3 hours (Fig. 5B). Unexpectedly, NAAD, NAMN, and NAR levels were also significantly increased (Fig. 5B and fig. S8A). Furthermore, the intravenous injection of NR and NMN efficiently increased NAD^+ levels in the skeletal muscle at 3 hours (Fig. 5C). Similar to that in the liver, the increase in NAAD, NAR, and NAMN levels was also observed in the skeletal muscle (Fig. 5C and fig. S8B). The increase of deamidated metabolites was unexpected because mammals, including humans and rodents, do not have deamidase, which converts NAM, NR, NMN, and NAD^+ to their deamidated forms (*26*–*28*). Therefore, we speculated that the gut microbiota was also involved in the generation of deamidated NAD^+ metabolome when NR and NMN were intravenously administered. Hence, we performed intravenous injection of NR and NMN to antibiotics (Abx)–treated mice to determine whether the deamidated NAD^+ metabolome was generated by the gut microbiota. The removal of the gut microbiota by Abx treatment completely suppressed the increase of NAAD, NAMN, and NAR in the liver after intravenous injection of NR and NMN (Fig. 5D and fig. S8C). In addition, the increase of NAD^+ was significantly suppressed in the liver of Abx-treated mice (Fig. 5D). In the skeletal muscle, the increase of NAAD, NAMN, and NAR was also completely suppressed by Abx treatment (Fig. 5E and fig. S8D). However, NAD^+ levels in the skeletal muscle were not affected by Abx treatment, suggesting that NAD^+ synthesis in the skeletal muscle was independent of the Preiss-Handler pathway (Fig. 5E). To confirm this, we performed the same experiments using *Naprt* KO mice. As expected, *Naprt* deletion did not affect NAD^+ levels, but suppressed deamidated intermediates in the skeletal muscle after the intravenous administration of NR and NMN (Fig. 5F and fig. S8E). On the other hand, the increase of NAD^+ metabolites except for NA in the liver was significantly suppressed in *Naprt* KO mice (Fig. 5G and fig. S8F). Furthermore, the levels of NR and NMN in the liver did not increase in *Naprt* KO mice when NR and NMN were intravenously administered (Fig. 5G). Accordingly, NAM levels did not increase in the liver of *Naprt* KO mice administered with NR or NMN, whereas the increase of NAM levels in the skeletal muscle were not suppressed in *Naprt* KO mice (Fig. 5, F and G). These data suggested that the gut microbiota plays an important role for NAD^+ synthesis in the liver during intravenous administration of NR and NMN.

Intravenously administered NR is converted to muscle NAD^+ via the salvage pathway

Intravenously injected NR and NMN could increase NAD^+ levels in the skeletal muscle of *Naprt* KO mice (Fig. 5F), suggesting that the salvage pathway is crucial for NAD^+ synthesis. We also found that intravenously injected NR and NMN were rapidly degraded to NAM and NR (Fig. 5A). Thus, we wish to determine whether intravenously injected NR can directly increase NAD^+ levels. To reveal the time course of NAD^+ metabolism when NR was intravenously injected into WT mice, we measured NAD^+ metabolome at 30 min and 3 hours after NR administration in the skeletal muscle and liver. We found that NAD^+ levels significantly increased at both time points (Fig. 6A and fig. S9). However, we only observed a significant rise of NR levels at 30 min, while NAAD levels significantly increased at 3 hours. Thus, we considered that NR reached the skeletal muscle at 30 min and directly converted to NAD^+. To examine this, we performed tracing experiments by intravenously injecting [m + 8] NR (Fig. 6B). In the liver, the increase in NAD^+ pool was mainly due to [m + 3], demonstrating that hydrolyzed [m + 3] NAM was used for the NAD^+ synthesis (Fig. 6, B and C, and fig. S10). On the other hand, we observed a significant rise of [m + 8] NR in the skeletal muscle, where although the major fractions for the increase in NAD^+ were [m + 0] and [m + 3], a certain amount of [m + 8] NAD^+ was also detected (Fig. 6D and fig. S11). These results suggested that intravenously injected NR could be directly converted to NAD^+ in the skeletal muscle, while some of it was degraded to NAM and then converted to NAD^+.

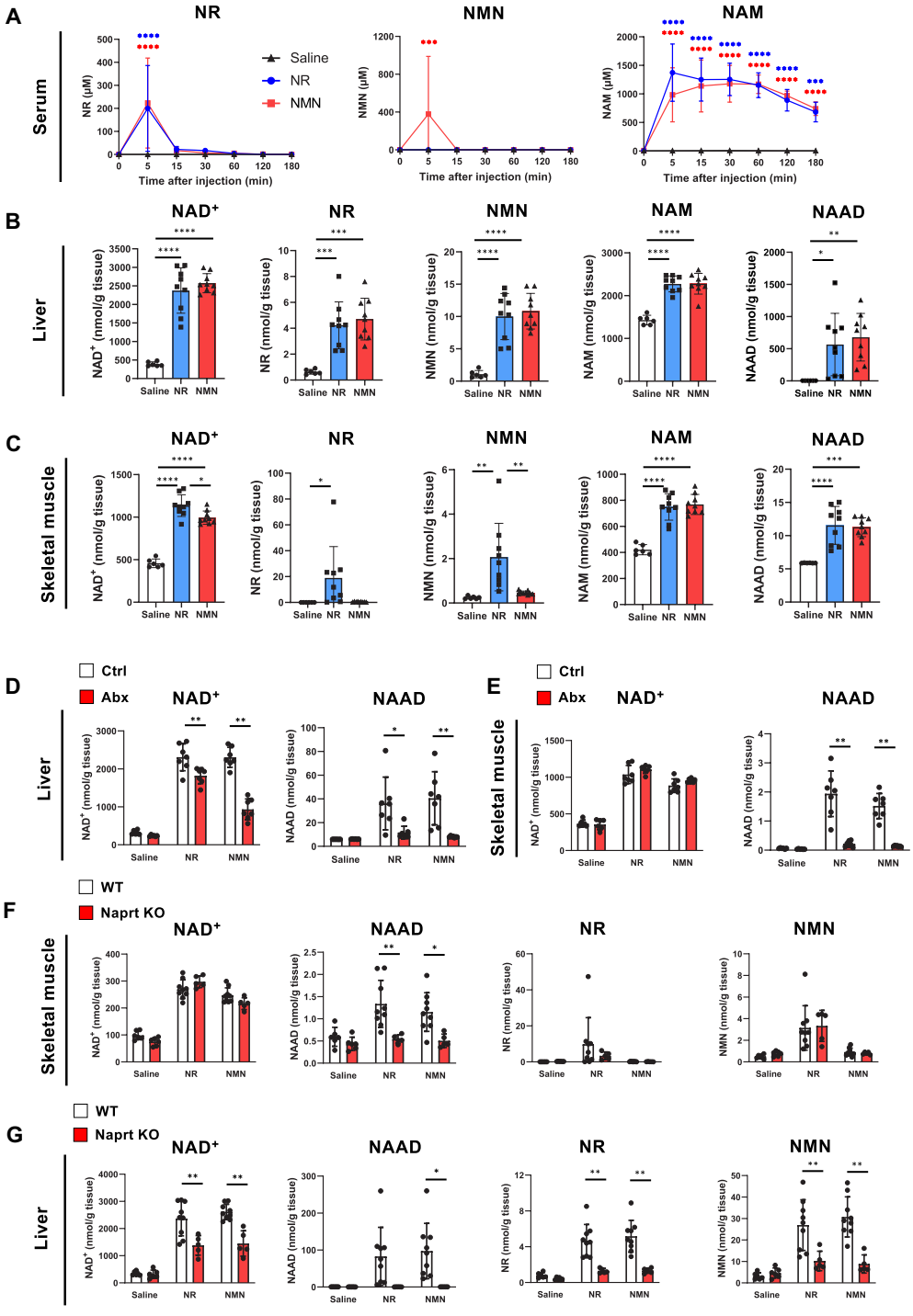

Fig. 5. Intravenous injection of NR and NMN elevated deamidated NAD$^+$ metabolites in the liver through gut microbiota. (**A**) Time course analysis of serum NAD$^+$ metabolome in mice intravenously injected with NMN and NR. $n = 6$ to 9 mice per group. P values of interaction effect; NR = 0.0002, NMN = 0.0018, and NAM < 0.0001. Asterisks indicate significance versus saline group at the same time point. (**B** and **C**) NAD$^+$ metabolome in the liver (B) and muscle (C) from WT mice at 3 hours after the intravenous injection of NMN and NR. $n = 6$ (saline group) and $n = 9$ (NR or NMN groups). (**D**) Liver NAD$^+$ metabolome in control and Abx-treated mice at 3 hours after the intravenous injection of NMN and NR. $n = 6$ to 7 mice per group. P values of interaction effect; NAD$^+$ < 0.0001, NAAD = 0.0118. (**E**) Muscle NAD$^+$ metabolome in control and Abx-treated mice at 3 hours after the intravenous injection of NMN and NR. $n = 6$ to 7 mice per group. P values of interaction effect; NAD$^+$ = 0.2939 and NAAD < 0.0001. (**F**) Muscle NAD$^+$ metabolome in WT and *Naprt* KO mice at 3 hours after the intravenous injection of NMN and NR. $n = 5$ to 9 mice per group. P values of interaction effect; NAD$^+$ = 0.0124, NAAD = 0.0792, NR = 0.4316, and NMN = 0.9108. (**G**) Liver NAD$^+$ metabolome in WT and *Naprt* KO mice at 3 hours after the intravenous injection of NMN and NR. $n = 5$ to 9 mice per group. P values of interaction effect; NAD$^+$ = 0.024, NAAD = 0.0622, NR = 0.0031, and NMN = 0.0016. Statistical significance was determined by Tukey's test (*P < 0.05, **P < 0.01, ***P < 0.001, and ****P < 0.0001).

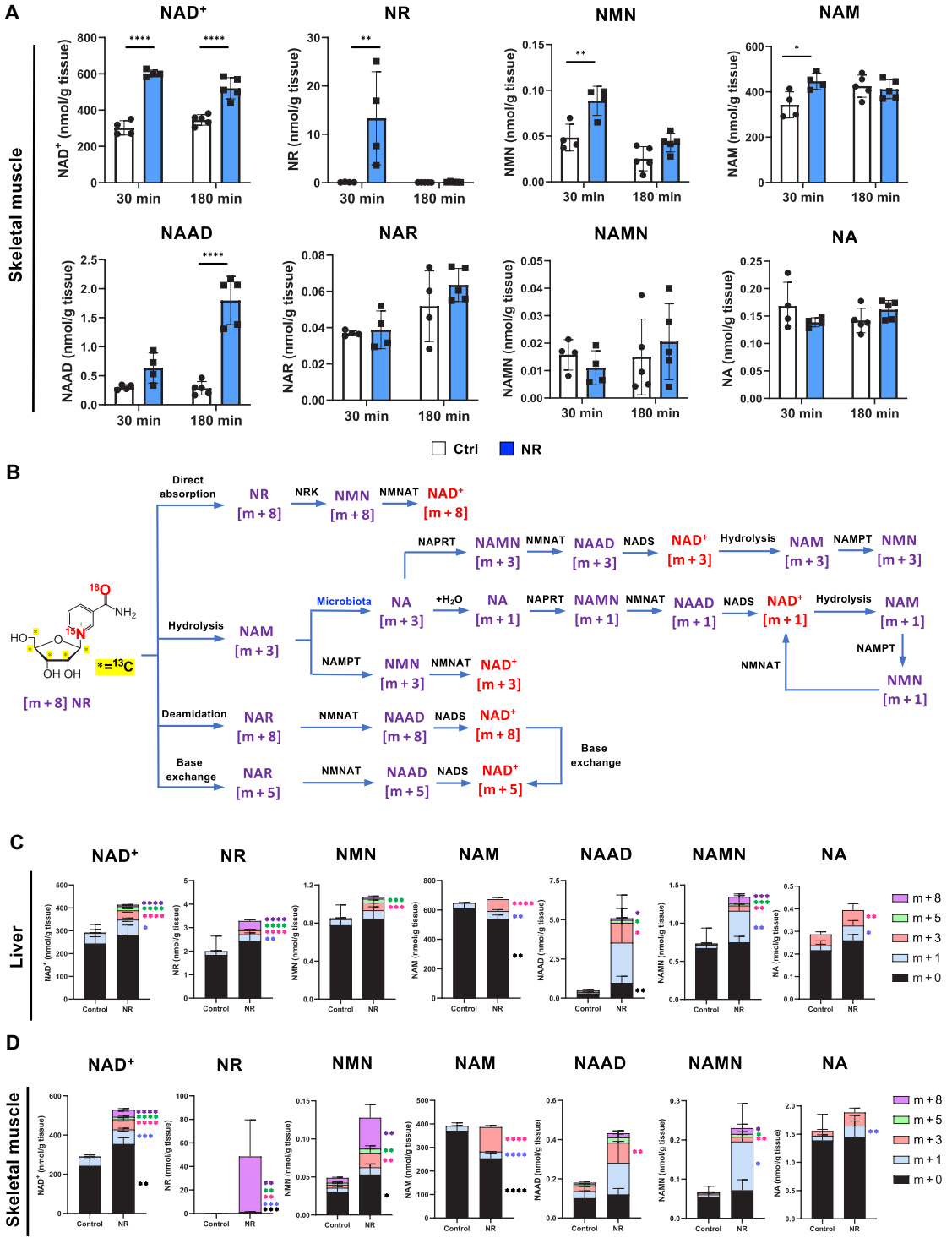

Fig. 6. NR is taken up by muscle and partially contributes to NAD$^+$ synthesis. (**A**) NAD$^+$ metabolome in muscle at 30 and 180 min after intravenous injection of non-labeled NR. $n = 4$ mice for 30 min and $n = 5$ mice for 180 min. NAD$^+$ = 0.0055, NR = 0.0078, NMN = 0.0960, NAM = 0.0187, NAAD = 0.0003, NAR = 0.4023, NAMN = 0.3484, and NA = 0.0604. Statistical significance was determined by Tukey's test (*$P < 0.05$, **$P < 0.01$, and ****$P < 0.0001$). (**B**) Scheme of formation of stable isotope–labeled NAD$^+$ metabolites after the oral administration of [m + 8] NR. (**C**) NAD$^+$ metabolome in the liver at 30 min after intravenous injection of [m + 8] NR. $n = 5$ mice for the control group and $n = 6$ mice for the NR-treated group. Statistical significance was determined by Student's t test (*$P < 0.05$, **$P < 0.01$, ***$P < 0.001$, and ****$P < 0.0001$). (**D**) NAD$^+$ metabolome in the muscle at 30 min after intravenous injection of [m + 8] NR. $n = 5$ mice for the control group and $n = 6$ mice for the NR-treated group. Statistical significance was determined by Student's t test (*$P < 0.05$, **$P < 0.01$, ***$P < 0.001$, and ****$P < 0.0001$).

Enterohepatic circulation of NAM and NR was involved in NAD^+ synthesis in the liver

Our results demonstrated that deamidated NAD^+ metabolites were generated depending on the gut microbiota even when NAD^+ precursors were intravenously injected. These findings suggested that the intravenously injected NAD^+ precursors were secreted to the gastrointestinal tract. However, the secretion route from the blood to the gastrointestinal tract remains unknown. Moreover, which forms of NAD^+ precursors were secreted to the gut when NR and NMN were intravenously administered remains to be elucidated. Generally, an excess amount of NAM is converted into *N*-methyl-2-pyridone-5-carboxamide (2-PY) or *N*-methyl-4-pyridone-5-carboxamide and then secreted from the kidney via urine. However, we speculated that bile is one possible route that comprises the metabolic cycle between the liver and the intestine. Therefore, we investigated whether bile is involved in the secretion of NAD^+ precursors to the intestinal lumen. We examined NAD^+ metabolites in the bile of WT mice under normal conditions and found that NR was the most abundant, followed by NAM and 2-PY (Fig. 7A). Next, we determined whether NR and NMN were secreted to the bile after intravenous injection. NAD^+ metabolome analysis revealed that intravenous injection of NR drastically increased NAM and NR levels, but not NMN (Fig. 7B). In turn, intravenous administration of NMN drastically increased NAM, but the increase of NMN was marginal (Fig. 7B). These data suggested that the enterohepatic circulation was the route for the secretion of NAD^+ precursors to the gut lumen from the blood and that NAM was the main form of secreted NAD^+ precursor. To confirm this, we intravenously injected d4-labeled NAM ([m + 4] NAM) and investigated the NAD^+ metabolome in the liver and bile (Fig. 7C). In the liver, the intravenous administration of d4-labeled NAM increased [m + 3]– and [m + 4]–labeled NAM, NAD^+, and NR, suggesting that NAM was rapidly converted to NR and NAD^+ (Fig. 7D). On the other hand, the [m + 4]–labeled fraction occupied the most part of NAM in the bile (Fig. 7E). In addition, the total pool of NR was not changed in the bile, whereas the [m + 4] fraction of NR was significantly increased by d4-labeled NAM injection (Fig. 7E). These results supported the concept that excess amount of NAM was rapidly secreted to the bile and converted to NA by the gut microbiota, followed by reabsorption from the large intestine. Last, we performed bile duct ligation (BDL) on WT mice to confirm the role of enterohepatic circulation in NAD^+ metabolism. BDL significantly suppressed the increase of NAAD (Fig. 7F). In addition, NAD^+ levels in the liver were decreased in bile duct–ligated mice when NMN was administered with a trend toward a significant interaction effect ($P = 0.0533$) (Fig. 7F). However, NAD^+ levels in the skeletal muscle were unaffected (Fig. 7G). These results suggested that enterohepatic circulation is an important route for NAD^+ synthesis in the liver.

DISCUSSION

In the present study, we comprehensively analyzed the NAD^+ synthesis pathways of orally and intravenously administered NMN and NR, demonstrating that most of NMN and NR were direct precursors of NAD^+ (Fig. 8). A previous study demonstrated that NMN was directly taken up to the small intestine via Slc12a8 (*32*). This study showed that the oral administration of stable isotope–labeled NMN, which was labeled on ribose and NAM moieties, rapidly increased the levels of double-labeled NMN in the jejunum and ileum of WT mice. However, this study could not rule out the possibility of indirect NMN transport after conversion to NR because the NMN labeling used in this study could not discriminate these possibilities. Our time course NAD^+ metabolomic data demonstrated that the oral administration of NMN, but not NR, rapidly increased intracellular NMN levels in the small intestine. Furthermore, the increase of NR after NMN administration was delayed compared with that of NR, suggesting that NMN was directly taken up (Fig. 1B). In addition, we found that A549 cells could rapidly uptake NMN without the increase of NR and that CD73 knockdown did not interfere with the increase of NAD^+ by NMN treatment. This finding suggested that cells can directly take up NMN. Another study demonstrated that CD73 could not dephosphorylate NMN to NR, but rather 5′-nucleotidase, cytosolic II (NT5C2) and 5′-nucleotidase, cytosolic III (NT5C3) were responsible for the conversion of NMN to NR (*43*, *44*). Therefore, examining the involvement of NT5C2 and NT5C3 in NMN metabolism in vivo is important. In addition, it is still unclear whether Slc12a8 is the only NMN transporter in mammals. Another transporter may be responsible for NMN uptake. The stable-isotope tracing experiment revealed that the contribution of NAD^+ synthesis directly from NMN was marginal. Further, NMN was rapidly degraded into NAM in the blood. Together, our kinetics study suggested that NMN is directly taken up from the small intestine, but only a limited amount of NMN is directly absorbed.

Our study suggested the existence of a route wherein certain NAD^+ intermediate metabolites are secreted to the intestinal tract. We demonstrated that NAM and NR were secreted into the bile after the intravenous administration of NMN and NR. They are also abundant in human breast milk and cow's milk (*45*–*47*). Thus, NAM and NR appear to be one of the external secretion forms of NAD^+ metabolites. However, the pathway by which NAM and NR were secreted to the bile remains unknown. Generally, NR is actively taken up via equilibrative nucleoside transporters (ENTs) (*29*, *48*). Thus, these ENTs are candidates involved in bile secretion. On the other hand, NAM has been considered to pass through the cytosolic membrane via passive diffusion (*49*, *50*). Therefore, excess NAM in the circulation was expected to reach the bile via the transcellular pathway through hepatocytes. When we intravenously administered d4-NAM, [m + 3] and [m + 4] NAM were increased in the liver. We speculated that [m + 3] NAM was derived from [m + 3] NAD^+ generated in hepatocytes. By contrast, the increased NAM in the bile was only the [m + 4]–labeled form. Therefore, circulating NAM might be transported via paracellular flux through the intercellular space. Further studies are needed to reveal the detailed mechanisms involved in the paracellular transport of NAM from the blood to the bile.

The biological advantage of the enterohepatic circulation of NAD^+ precursors might be niacin preservation. If NAM was disposed to urine, it could not be reused by other tissues. However, the liver can reuse NAM when there is excess amount of NAM intake. Moreover, the liver prefers NA rather than NAM, and the enterohepatic circulation also facilitates the conversion of NAM into NA by the gut microbiota. It is unknown why the liver did not preferentially use amidated metabolites, including NAM, NR, and NMN, for NAD^+ synthesis. One of the important roles of the liver in NAD^+ metabolism is to supply NAM to other peripheral organs, including the skeletal muscle (*40*, *51*). In glucose metabolism, the liver synthesizes rather than catabolizes glucose (*52*). To reduce glucose utilization, hepatic glucokinase is known to have a higher K_m value against

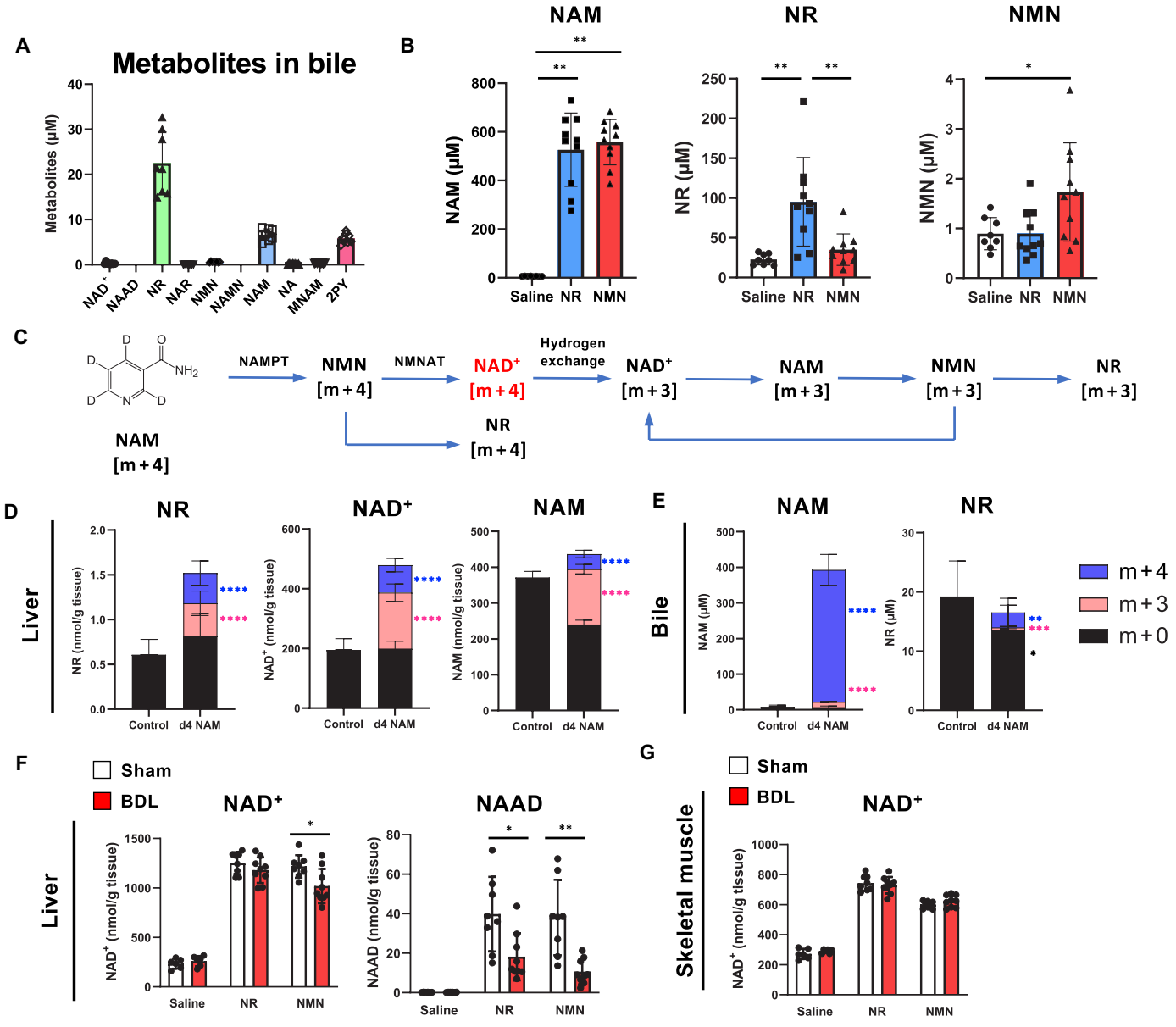

Fig. 7. Enterohepatic circulation of NAD^+ precursors was important for NAD^+ synthesis in the liver. (**A**) NAD^+ metabolome in the bile of WT mice under normal conditions. $n = 8$ mice. (**B**) NAD^+ metabolome in the bile of WT mice at 30 min after the intravenous injection of NMN and NR. $n = 8$ to 10 mice per group. Statistical significance was determined by Tukey's test (*$P < 0.05$ and **$P < 0.01$). (**C**) Scheme of formation of stable isotope–labeled NAD^+ metabolites after the intravenous injection of [m + 4] NAM. (**D**) NAD^+ metabolome in the liver of WT mice at 30 min after the intravenous injection of [m + 4] NAM. $n = 8$ mice for saline group and $n = 11$ mice for NAM-treated group. Statistical significance was determined by Student's t test (****$P < 0.0001$). (**E**) NAD^+ metabolome in the bile of WT mice at 30 min after the intravenous injection of [m + 4] NAM. $n = 8$ mice for the saline group and $n = 10$ mice for the NAM-treated group. Statistical significance was determined by Student's t test (*$P < 0.05$, **$P < 0.01$, ***$P < 0.001$, and ****$P < 0.0001$). (**F**) NAD^+ metabolome in the liver of sham- and bile duct ligation (BDL)–operated mice at 3 hours after the intravenous injection of NMN and NR. $n = 6$ to 9 mice per group. P values of interaction effect; $NAD^+ = 0.0533$ and NAAD = 0.0201. Statistical significance was determined by Tukey's test (*$P < 0.05$ and **$P < 0.01$). (**G**) NAD^+ levels in the skeletal muscle of sham- and BDL-operated mice at 3 hours after the intravenous injection of NMN and NR. $n = 6$ to 9 mice per group. P values of interaction effect; $NAD^+ = 0.3869$. Statistical significance was determined by Tukey's test.

glucose than glucokinases in other tissues (*53*, *54*). Thus, it is interesting to examine whether hepatic NAMPT has low affinity to NAM compared with other tissues. The secretion of NAM to the intestinal lumen may also foster the gut microbiota. The oral administration of NAD^+ precursors is known to alter the gut microbiota composition (*55*–*59*). Thus, the continuous circulation of NAD^+ precursors may be helpful for maintaining the proper composition of the gut microbiota.

Limitations of the study

In this study, we analyzed the fate of NR and NMN in vivo using single oral gavage and intravenous injection. A previous study proposed

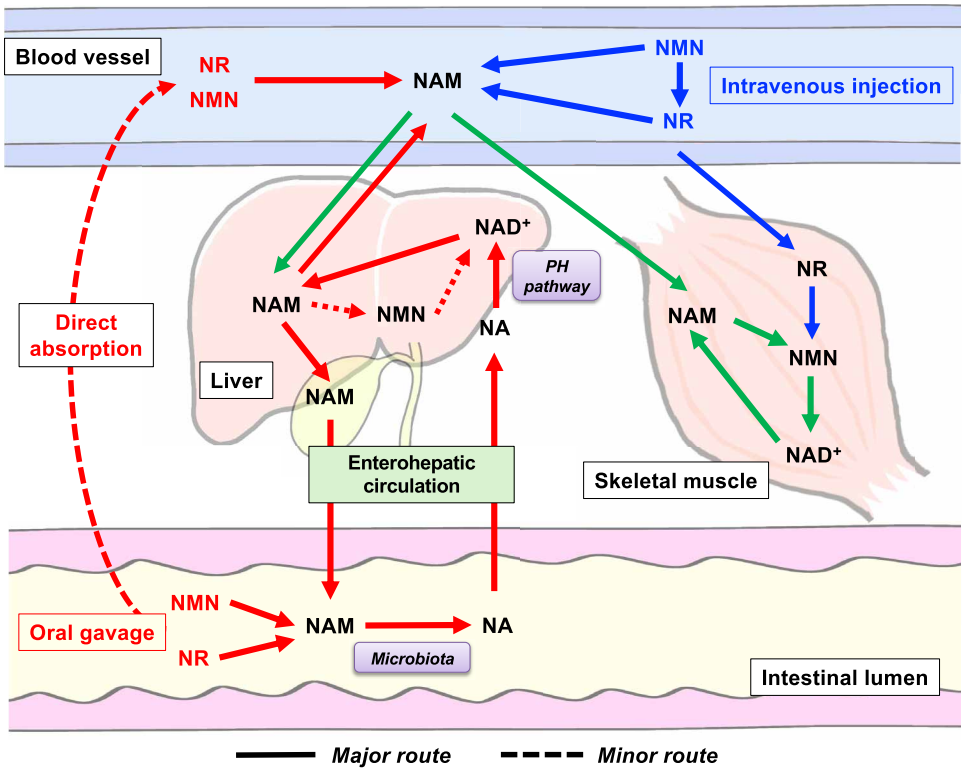

Fig. 8. Overview of NAD$^+$ metabolism in the liver and skeletal muscle after oral and intravenous administration of NMN and NR. The metabolic pathways of orally administered NMN and NR are noted in red, and those of intravenously administered NMN and NR are noted in blue. The shared pathways are in green. The solid and dashed lines note the major and minor routes, respectively.

that orally administered NR was directly absorbed from the intestine as an intact form and converted to NMN by NRK inside cells (*11*, *60*). However, subsequent studies and our current study demonstrated that orally administered NR was degraded into NAM and then converted to NA by gut microbiota before absorption (*22*–*24*). On the other hand, our current study found that a significant amount of intravenously injected NR could be directly converted to NAD$^+$ in the skeletal muscle (Fig. 6D). This finding suggests that intravenous injection of NR may be a therapeutic option that effectively increases NAD$^+$ levels in skeletal muscle. Further, it remains unknown whether oral administration of NMN and NR contributes to a rise of NAD$^+$ levels via the direct NAD$^+$ synthesis pathway during the long-term administration. A previous study demonstrated that intravenous injections of NR for 4 weeks increased NAD$^+$ levels, although NRK2 expression in skeletal muscle is significantly down-regulated (*61*). This suggests that the skeletal muscle suppressed the direct NAD$^+$ synthesis from NR during long-term administration of NR. However, it is also a fact that certain amounts of NR and NMN were directly absorbed through their administration. Thus, direct NAD$^+$ synthesis from NR or NMN may contribute to a rise in NAD$^+$ levels during long-term administration. Accordingly, the therapeutic advantage of NR and NMN during long-term administration should be clarified using GF mice and *Naprt* KO mice.

In addition, it remains unclear whether in vivo NAD$^+$ metabolism in humans is the same as that in mice. Previously, we conducted human clinical trials examining the safety and efficacy of NMN and found that NAMN levels were significantly increased after NMN administration (*62*). This result implies that orally administered NMN is degraded to NA in humans. However, further studies are needed to clarify NMN and NR metabolism in humans to improve their use for NAD$^+$ replenishment therapy.

MATERIALS AND METHODS

Animals

C57BL/6N mice were obtained from Japan SLC Inc. (Shizuoka, Japan). *Naprt* KO mice were generated as previously described (*22*). The GF C57BL/6 mice were housed in vinyl isolators and obtained by natural mating. The feces of GF mice, wood chip bedding, and cotton-wiped isolators were tested for sterility at the Central Institute for Experimental Animals (Kanawaga, Japan) once a month. Animals were fed a standard chow diet (Nosan Corporation, Yokohama, Japan) with free access to water. All the animals were kept under a controlled temperature and standard light condition (a 12-hour light/12-hour dark cycle). All the animal experiments were approved by the Animal Experiment Committee at the University of Toyama and were performed in accordance with the Guidelines for the Care and Use of Laboratory Animals at the University of Toyama, which are based on international policies (approval no. A2022MED-19).

NAD$^+$ precursor treatment

For single gavage experiments, 1.57 mmol NR chloride (456 mg) (Angene Chemical, AG01DJ4H) per kilogram of body weight or 1.57 mmol NMN (524 mg) (Angene Chemical, AG003880) per kilogram of body weight was given to 8- to 10-week-old male C57BL/6N mice. NAD$^+$ precursors administered to animals were diluted in saline,

and the same volume of saline was used as a control. For long-term gavage experiments, 131 mg of NMN per kilogram of body weight or equivalent mole amount of NMN was given to mice for 2 weeks. NAD^+ precursors administered to animals were diluted in saline, and the same volume of saline was used as a control. For intravenous injection experiments, mice were injected with 1.57 mmol NR chloride (456 mg), 1.57 mmol NMN (524 mg), or 1.57 mmol [m + 4] NAM (198 mg) (CDN isotopes, D-3457) via lateral tail vein injection. At the end of the experiment, tissues were collected and immediately frozen in liquid nitrogen and kept at −80°C until use.

Abx treatment

For Abx treatment, mice were given either regular water or autoclaved water containing Abx cocktail of vancomycin (0.5 g/liter, LKT LAB, St. Paul, MN, USA), ampicillin (1 g/liter), metronidazole (1 g/liter, Sigma-Aldrich), and neomycin (1 g/liter, Sigma-Aldrich) for 3 days.

Bile duct ligation

For bile duct ligation, mice were anesthetized with an intraperitoneal injection of a mixture of three drugs [medetomidine hydrochloride (0.75 mg/kg), midazolam (4 mg/kg), and butorphanol tartrate (5 mg/kg)]. Subsequent to deletion of pain response, abdomen was opened along midline. A 5-0 medical suture was used to ligate the common bile duct at two spots. After the operation, 456 mg of NR or equivalent mole amount of NMN was injected intravenously. To avoid hypothermia, atipamezole hydrochloride (0.375 mg/kg) was intraperitoneally injected and mice were kept on heat pad until sacrifice.

Cell culture

A549 cells were cultured in Dulbecco's modified Eagle's medium supplemented with 10% fetal bovine serum at 37°C under a gas phase of 95% air and 5% CO_2. Cells were seeded at 2.5×10^5 cells per well in a 12-well plate 1 day before treatment. The next day, cells were treated with NMN at a concentration of 500 or 250 μM for different time points. After the treatment, cells were washed with saline twice, and ice-cold 50% methanol–50% water was added followed by the harvest using a cell scraper.

Small interfering RNA

For the small interfering RNA (siRNA) treatment, A549 cells were seeded in six-well plates at 1.5×10^5 per well and cultured 24 hours with DMEM containing 10% FBS. Then, the cells were transfected with siRNAs using 5 μl of Lipofectamine RNAiMAX (Thermo Fisher Scientific) and 5 pmol of siRNA in 500 μl of Opti-MEM (Thermo Fisher Scientific). siGENOME SMART pool Human NT5E siRNA (siGENOME Nt5e siRNA; catalog no. M-008217-00) and siGENOME Non-Targeting siRNA Control Pools (catalog no. D-001206-130) were obtained from Dharmacon. The treated cells were incubated for 2 days and then were subjected to the subsequent experiments.

NAD^+ metabolomics

Metabolite extraction and NAD^+ metabolomics were performed as previously described (*63*). In this study, the gastrocnemius muscle was used as the skeletal muscle. Tissues were ground in ice-cold 50% methanol–50% water at concentrations of 50 mg tissue/ml by using a multi-beads shocker (Yasui Kikai, Japan) under optimal conditions. Subsequently, 600 μl of lysate was mixed with 600 μl of chloroform and the mixture was vortexed for 10 s. The mixture was centrifuged at 13,000*g* for 10 min at 4°C. The upper phase (aqueous phase) was collected into another tube, and the same procedures were repeated. Then, the transferred aqueous phase was dried by using a SpeedVac SPD1010 (Thermo Fisher Scientific). Last, the dried samples were reconstituted in liquid chromatography–mass spectrometry grade water (FUJIFILM Wako Pure Chemical Corporation, Osaka, Japan) and filtered with 0.45 μm Millex filter unit (Merck ltd. Tokyo, Japan) before the injection. Metabolites were analyzed by the Agilent 6460 Triple Quad mass spectrometer coupled with the Agilent 1290 HPLC system. Analytes were separated by Atlantis T3 Column (2.1 × 150 mm, particle size 3 μm, Waters) using mobile phase A (5 mM ammonium formate) and mobile phase B (methanol) with a flow rate of 150 μl/min and a column temperature of 40°C. The programmed mobile phase gradient was as follows: 0 to 10 min, 0 to 70% B; 10 to 15 min, 70% B; 15 to 20 min, 0% B. Data were analyzed by MassHunter Quantitative analysis software (Agilent) and quantifications were performed by using the standard curve obtained from various concentrations of standard compounds. Detection of labeled NAD^+ metabolites was performed by using modulated transitions of mass/charge ratio, equal fragmentor voltage, and equal collision energy with nonlabeled NAD^+ metabolites.

Synthesis of [m + 8] NMN and [m + 8] NR

Synthesis of [m + 6] NR was described elsewhere (*22*). [m + 5] D-ribose and [m + 3] NAM were prepared according to previously reported procedure (*64*, *65*). A synthesis scheme of [m + 8] NMN and [m + 8] NR is shown in the Supplementary Materials.

Western blot analysis

Cell lysates were prepared from A549 cells by sonicating in RIPA buffer (500 mM NaCl, 1% Nonidet P-40, 0.5% sodium deoxycholate, 0.1% SDS, and 50 mM tris-HCl, pH 7.4). After centrifugation, the supernatant was mixed with sample buffer and denatured by boiling at 95°C for 5 min. Proteins were separated on a 10% polyacrylamide gel and transferred to a PVDF Immobilon-P membrane (Millipore, MA, USA). The membrane was blocked with 5% skim milk and incubated overnight at 4°C with primary antibodies and then for 1 hour at room temperature with secondary antibodies. Chemiluminescence was detected using Chemi-Lumi One Super (Nacalai Tesque, Kyoto, Japan), and images were captured with a LAS 4000 Mini digital imager (GE Healthcare, Tokyo, Japan). The antibodies used included anti-NT5E/CD73 (CST, catalog no. 13160, MA, Japan), anti–γ-actin (Wako, catalog no. 010-27841, Osaka, Japan), anti-rabbit immunoglobulin G (IgG; CST, catalog no. 7074), and anti-mouse IgG (CST, catalog no. 7076).

Statistical analysis

Data are expressed as means ± SD. Data were analyzed using Prism software (version 9.5.1, GraphPad Software, San Diego, CA, USA). *P* values less than 0.05 were determined as statistically significant. *P* values in the range of 0.05 to 0.1 were interpreted as trends, indicating a possible but not statistically confirmed effect. The significant differences between two groups were analyzed by Student's two-tailed *t* test. The significant differences among more than two groups were evaluated by one-way analysis of variance (ANOVA), two-way ANOVA, two-way ANOVA repeated measures, or a mixed-effects model. Tukey's post hoc tests followed if *P* value of ANOVA is significant or shows a trend. Additional one-way ANOVA with Tukey's

test was performed separately at each factor if the main group effect was significant ($P < 0.05$) to determine the effects that are particularly relevant to the biological context.

Supplementary Materials

This PDF file includes:
Figs. S1 to S11
Supplementary Method

REFERENCES AND NOTES

1. K. Yaku, T. Nakagawa, NAD$^+$ precursors in human health and disease: Current status and future prospects. *Antioxid. Redox Signal.* **39**, 1133–1149 (2023).
2. J. Camacho-Pereira, M. G. Tarragó, C. C. S. Chini, V. Nin, C. Escande, G. M. Warner, A. S. Puranik, R. A. Schoon, J. M. Reid, A. Galina, E. N. Chini, CD38 dictates age-related nad decline and mitochondrial dysfunction through an SIRT3-dependent mechanism. *Cell Metab.* **23**, 1127–1139 (2016).
3. T. Iqbal, T. Nakagawa, The therapeutic perspective of NAD$^+$ precursors in age-related diseases. *Biochem. Biophys. Res. Commun.* **702**, 149590 (2024).
4. J. Yoshino, J. A. Baur, S.-I. Imai, NAD$^+$ intermediates: The biology and therapeutic potential of NMN and NR. *Cell Metab.* **27**, 513–528 (2018).
5. K. Yaku, K. Okabe, T. Nakagawa, NAD metabolism: Implications in aging and longevity. *Ageing Res. Rev.* **47**, 1–17 (2018).
6. K. Hikosaka, K. Yaku, K. Okabe, T. Nakagawa, Implications of NAD metabolism in pathophysiology and therapeutics for neurodegenerative diseases. *Nutr. Neurosci.* **24**, 371–383 (2021).
7. K. Okabe, K. Yaku, K. Tobe, T. Nakagawa, Implications of altered NAD metabolism in metabolic disorders. *J. Biomed. Sci.* **26**, 34 (2019).
8. S. U. Rahman, A. Qadeer, Z. Wu, Role and potential mechanisms of nicotinamide mononucleotide in aging. *Aging Dis.* **15**, 565–583 (2024).
9. L. Rajman, K. Chwalek, D. A. Sinclair, Therapeutic potential of NAD-boosting molecules: The in vivo evidence. *Cell Metab.* **27**, 529–547 (2018).
10. J. R. Revollo, A. A. Grimm, S.-I. Imai, The NAD biosynthesis pathway mediated by nicotinamide phosphoribosyltransferase regulates Sir2 activity in mammalian cells. *J. Biol. Chem.* **279**, 50754–50763 (2004).
11. J. Ratajczak, M. Joffraud, S. A. Trammell, R. Ras, N. Canela, M. Boutant, S. S. Kulkarni, M. Rodrigues, P. Redpath, M. E. Migaud, J. Auwerx, O. Yanes, C. Brenner, C. Cantó, NRK1 controls nicotinamide mononucleotide and nicotinamide riboside metabolism in mammalian cells. *Nat. Commun.* **7**, 13103 (2016).
12. P. Belenky, K. C. Christensen, F. Gazzaniga, A. A. Pletnev, C. Brenner, Nicotinamide riboside and nicotinic acid riboside salvage in fungi and mammals. Quantitative basis for Urh1 and purine nucleoside phosphorylase function in NAD$^+$ metabolism. *J. Biol. Chem.* **284**, 158–164 (2009).
13. J. Yoshino, K. F. Mills, M. J. Yoon, S. Imai, Nicotinamide mononucleotide, a key NAD$^+$ intermediate, treats the pathophysiology of diet- and age-induced diabetes in mice. *Cell Metab.* **14**, 528–536 (2011).
14. C. Cantó, R. H. Houtkooper, E. Pirinen, D. Y. Youn, M. H. Oosterveer, Y. Cen, P. J. Fernandez-Marcos, H. Yamamoto, P. A. Andreux, P. Cettour-Rose, K. Gademann, C. Rinsch, K. Schoonjans, A. A. Sauve, J. Auwerx, The NAD$^+$ precursor nicotinamide riboside enhances oxidative metabolism and protects against high-fat diet-induced obesity. *Cell Metab.* **15**, 838–847 (2012).
15. V. Sorrentino, M. Romani, L. Mouchiroud, J. S. Beck, H. Zhang, D. D'Amico, N. Moullan, F. Potenza, A. W. Schmid, S. Rietsch, S. E. Counts, J. Auwerx, Enhancing mitochondrial proteostasis reduces amyloid-β proteotoxicity. *Nature* **552**, 187–193 (2017).
16. M. J. Bertoldo, D. R. Listijono, W. J. Ho, A. H. Riepsamen, D. M. Goss, D. Richani, X. L. Jin, S. Mahbub, J. M. Campbell, A. Habibalahi, W. N. Loh, N. A. Youngson, J. Maniam, A. S. A. Wong, K. Selesniemi, S. Bustamante, C. Li, Y. Zhao, M. B. Marinova, L. J. Kim, L. Lau, R. M. Wu, A. S. Mikolaizak, T. Araki, D. G. Le Couteur, N. Turner, M. J. Morris, K. A. Walters, E. Goldys, C. O'Neill, R. B. Gilchrist, D. A. Sinclair, H. A. Homer, L. E. Wu, NAD$^+$ repletion rescues female fertility during reproductive aging. *Cell Rep.* **30**, 1670–1681.e7 (2020).
17. K. F. Mills, S. Yoshida, L. R. Stein, A. Grozio, S. Kubota, Y. Sasaki, P. Redpath, M. E. Migaud, R. S. Apte, K. Uchida, J. Yoshino, S. I. Imai, Long-term administration of nicotinamide mononucleotide mitigates age-associated physiological decline in mice. *Cell Metab.* **24**, 795–806 (2016).
18. M. Yoshino, J. Yoshino, B. D. Kayser, G. J. Patti, M. P. Franczyk, K. F. Mills, M. Sindelar, T. Pietka, B. W. Patterson, S. I. Imai, S. Klein, Nicotinamide mononucleotide increases muscle insulin sensitivity in prediabetic women. *Science* **372**, 1224–1229 (2021).
19. B. Brakedal, C. Dölle, F. Riemer, Y. Ma, G. S. Nido, G. O. Skeie, A. R. Craven, T. Schwarzlmüller, N. Brekke, J. Diab, L. Sverkeli, V. Skjeie, K. Varhaug, O. B. Tysnes, S. Peng, K. Haugarvoll, M. Ziegler, R. Grüner, D. Eidelberg, C. Tzoulis, The NADPARK study: A randomized phase I trial of nicotinamide riboside supplementation in Parkinson's disease. *Cell Metab.* **34**, 396–407.e6 (2022).
20. O. L. Dollerup, S. Chubanava, M. Agerholm, S. D. Søndergård, A. Altıntaş, A. B. Møller, K. F. Høyer, S. Ringgaard, H. Stødkilde-Jørgensen, G. G. Lavery, R. Barrès, S. Larsen, C. Prats, N. Jessen, J. T. Treebak, Nicotinamide riboside does not alter mitochondrial respiration, content or morphology in skeletal muscle from obese and insulin-resistant men. *J. Physiol.* **598**, 731–754 (2020).
21. H. Akasaka, H. Nakagami, K. Sugimoto, Y. Yasunobe, T. Minami, T. Fujimoto, K. Yamamoto, C. Hara, A. Shiraki, K. Nishida, K. Asano, M. Kanou, K. Yamana, S. I. Imai, H. Rakugi, Effects of nicotinamide mononucleotide on older patients with diabetes and impaired physical performance: A prospective, placebo-controlled, double-blind study. *Geriatr. Gerontol. Int.* **23**, 38–43 (2023).
22. K. Yaku, S. Palikhe, H. Izumi, T. Yoshida, K. Hikosaka, F. Hayat, M. Karim, T. Iqbal, Y. Nitta, A. Sato, M. E. Migaud, K. Ishihara, H. Mori, T. Nakagawa, BST1 regulates nicotinamide riboside metabolism via its glycohydrolase and base-exchange activities. *Nat. Commun.* **12**, 6767 (2021).
23. I. Shats, J. G. Williams, J. Liu, M. V. Makarov, X. Wu, F. B. Lih, L. J. Deterding, C. Lim, X. Xu, T. A. Randall, E. Lee, W. Li, W. Fan, J. L. Li, M. Sokolsky, A. V. Kabanov, L. Li, M. E. Migaud, J. W. Locasale, X. Li, Bacteria boost mammalian host NAD metabolism by engaging the deamidated biosynthesis pathway. *Cell Metab.* **31**, 564–579.e7 (2020).
24. K. Chellappa, M. R. McReynolds, W. Lu, X. Zeng, M. Makarov, F. Hayat, S. Mukherjee, Y. R. Bhat, S. R. Lingala, R. T. Shima, H. C. Descamps, T. Cox, L. Ji, C. Jankowski, Q. Chu, S. M. Davidson, C. A. Thaiss, M. E. Migaud, J. D. Rabinowitz, J. A. Baur, NAD precursors cycle between host tissues and the gut microbiome. *Cell Metab.* **34**, 1947–1959.e5 (2022).
25. F. Gazzaniga, R. Stebbins, S. Z. Chang, M. A. McPeek, C. Brenner, Microbial NAD metabolism: Lessons from comparative genomics. *Microbiol. Mol. Biol. Rev.* **73**, 529–541 (2009).
26. G. Wang, E. Pichersky, Nicotinamidase participates in the salvage pathway of NAD biosynthesis in Arabidopsis. *Plant J.* **49**, 1020–1029 (2007).
27. M. Di Stefano, I. Nascimento-Ferreira, G. Orsomando, V. Mori, J. Gilley, R. Brown, L. Janeckova, M. E. Vargas, L. A. Worrell, A. Loreto, J. Tickle, J. Patrick, J. R. Webster, M. Marangoni, F. M. Carpi, S. Pucciarelli, F. Rossi, W. Meng, A. Sagasti, R. R. Ribchester, G. Magni, M. P. Coleman, L. Conforti, A rise in NAD precursor nicotinamide mononucleotide (NMN) after injury promotes axon degeneration. *Cell Death Differ.* **22**, 731–742 (2015).
28. S. Feng, L. Guo, H. Wang, S. Yang, H. Liu, Bacterial PncA improves diet-induced NAFLD in mice by enabling the transition from nicotinamide to nicotinic acid. *Commun. Biol.* **6**, 235 (2023).
29. A. Nikiforov, C. Dölle, M. Niere, M. Ziegler, Pathways and subcellular compartmentation of NAD biosynthesis in human cells: From entry of extracellular precursors to mitochondrial NAD generation. *J. Biol. Chem.* **286**, 21767–21778 (2011).
30. S. Garavaglia, S. Bruzzone, C. Cassani, L. Canella, G. Allegrone, L. Sturla, E. Mannino, E. Millo, A. De Flora, M. Rizzi, The high-resolution crystal structure of periplasmic *Haemophilus influenzae* NAD nucleotidase reveals a novel enzymatic function of human CD73 related to NAD metabolism. *Biochem. J.* **441**, 131–141 (2012).
31. A. Grozio, G. Sociali, L. Sturla, I. Caffa, D. Soncini, A. Salis, N. Raffaelli, A. De Flora, A. Nencioni, S. Bruzzone, CD73 protein as a source of extracellular precursors for sustained NAD$^+$ biosynthesis in FK866-treated tumor cells. *J. Biol. Chem.* **288**, 25938–25949 (2013).
32. A. Grozio, K. F. Mills, J. Yoshino, S. Bruzzone, G. Sociali, K. Tokizane, H. C. Lei, R. Cunningham, Y. Sasaki, M. E. Migaud, S. I. Imai, Slc12a8 is a nicotinamide mononucleotide transporter. *Nat. Metab.* **1**, 47–57 (2019).
33. L. J. Kim, T. J. Chalmers, R. Madawala, G. C. Smith, C. Li, A. Das, E. W. K. Poon, J. Wang, S. P. Tucker, D. A. Sinclair, L. E. Quek, L. E. Wu, Host-microbiome interactions in nicotinamide mononucleotide (NMN) deamidation. *FEBS Lett.* **597**, 2196–2220 (2023).
34. H. Zhang, D. Ryu, Y. Wu, K. Gariani, X. Wang, P. Luan, D. D'Amico, E. R. Ropelle, M. P. Lutolf, R. Aebersold, K. Schoonjans, K. J. Menzies, J. Auwerx, NAD$^+$ repletion improves mitochondrial and stem cell function and enhances life span in mice. *Science* **352**, 1436–1443 (2016).
35. D. W. Frederick, E. Loro, L. Liu, A. Davila Jr., K. Chellappa, I. M. Silverman, W. J. Quinn III, S. J. Gosai, E. D. Tichy, J. G. Davis, F. Mourkioti, B. D. Gregory, R. W. Dellinger, P. Redpath, M. E. Migaud, E. Nakamaru-Ogiso, J. D. Rabinowitz, T. S. Khurana, J. A. Baur, Loss of NAD homeostasis leads to progressive and reversible degeneration of skeletal muscle. *Cell Metab.* **24**, 269–282 (2016).
36. G. E. Janssens, L. Grevendonk, R. Z. Perez, B. V. Schomakers, J. de Vogel-van n Bosch, J. M. W. Geurts, M. van Weeghel, P. Schrauwen, R. H. Houtkooper, J. Hoeks, Healthy aging and muscle function are positively associated with NAD$^+$ abundance in humans. *Nat. Aging.* **2**, 254–263 (2022).
37. A. L. Basse, M. Agerholm, J. Farup, E. Dalbram, J. Nielsen, N. Ørtenblad, A. Altıntaş, A. M. Ehrlich, T. Krag, S. Bruzzone, M. Dall, R. M. de Guia, J. B. Jensen, A. B. Møller, A. Karlsen, M. Kjær, R. Barrès, J. Vissing, S. Larsen, N. Jessen, J. T. Treebak, Nampt controls skeletal muscle development by maintaining Ca^{2+} homeostasis and mitochondrial integrity. *Mol. Metab.* **53**, 101271 (2021).

38. M. Agerholm, M. Dall, B. A. H. Jensen, C. Prats, S. Madsen, A. L. Basse, A. S. Graae, S. Risis, J. Goldenbaum, B. Quistorff, S. Larsen, S. G. Vienberg, J. T. Treebak, Perturbations of NAD^+ salvage systems impact mitochondrial function and energy homeostasis in mouse myoblasts and intact skeletal muscle. *Am. J. Physiol. Endocrinol. Metab.* **314**, E377–E395 (2018).
39. Y. S. Elhassan, K. Kluckova, R. S. Fletcher, M. S. Schmidt, A. Garten, C. L. Doig, D. M. Cartwright, L. Oakey, C. V. Burley, N. Jenkinson, M. Wilson, S. J. E. Lucas, I. Akerman, A. Seabright, Y. C. Lai, D. A. Tennant, P. Nightingale, G. A. Wallis, K. N. Manolopoulos, C. Brenner, A. Philp, G. G. Lavery, Nicotinamide riboside augments the aged human skeletal muscle NAD(+) metabolome and induces transcriptomic and anti-inflammatory signatures. *Cell Rep.* **28**, 1717–1728.e6 (2019).
40. L. Liu, X. Su, W. J. Quinn III, S. Hui, K. Krukenberg, D. W. Frederick, P. Redpath, L. Zhan, K. Chellappa, E. White, M. Migaud, T. J. Mitchison, J. A. Baur, J. D. Rabinowitz, Quantitative analysis of NAD synthesis-breakdown fluxes. *Cell Metab.* **27**, 1067–1080.e5 (2018).
41. J. Giroud-Gerbetant, M. Joffraud, M. P. Giner, A. Cercillieux, S. Bartova, M. V. Makarov, R. Zapata-Pérez, J. L. Sánchez-García, R. H. Houtkooper, M. E. Migaud, S. Moco, C. Canto, A reduced form of nicotinamide riboside defines a new path for NAD^+ biosynthesis and acts as an orally bioavailable NAD^+ precursor. *Mol. Metab.* **30**, 192–202 (2019).
42. R. Zapata-Pérez, A. Tammaro, B. V. Schomakers, A. M. L. Scantlebery, S. Denis, Elfrink, H. L., J. Giroud-Gerbetant, C. Cantó, C. López-Leonardo, R. L. McIntyre, M. van Weeghel, Á. Sánchez-Ferrer, R. H. Houtkooper, Reduced nicotinamide mononucleotide is a new and potent NAD^+ precursor in mammalian cells and mice. *FASEB J.* **35**, e21456 (2021).
43. A. Wilk, F. Hayat, R. Cunningham, J. Li, S. Garavaglia, L. Zamani, D. M. Ferraris, P. Sykora, J. Andrews, J. Clark, A. Davis, L. Chaloin, M. Rizzi, M. Migaud, R. W. Sobol, Extracellular NAD^+ enhances PARP-dependent DNA repair capacity independently of CD73 activity. *Sci. Rep.* **10**, 651 (2020).
44. V. Kulikova, K. Shabalin, K. Nerinovski, C. Dölle, M. Niere, A. Yakimov, P. Redpath, M. Khodorkovskiy, M. E. Migaud, M. Ziegler, A. Nikiforov, Generation, release, and uptake of the NAD precursor nicotinic acid riboside by human cells. *J. Biol. Chem.* **290**, 27124–27137 (2015).
45. P. Bieganowski, C. Brenner, Discoveries of nicotinamide riboside as a nutrient and conserved NRK genes establish a Preiss-Handler independent route to NAD^+ in fungi and humans. *Cell* **117**, 495–502 (2004).
46. S. A. Trammell, L. Yu, P. Redpath, M. E. Migaud, C. Brenner, Nicotinamide riboside is a major NAD^+ precursor vitamin in cow milk. *J. Nutr.* **146**, 957–963 (2016).
47. K. Redeuil, J. Vulcano, F. P. Prencipe, S. Bénet, E. Campos-Giménez, M. Meschiari, First quantification of nicotinamide riboside with B_3 vitamers and coenzymes secreted in human milk by liquid chromatography-tandem-mass spectrometry. *J. Chromatogr. B Analyt. Technol. Biomed. Life Sci.* **1110–1111**, 74–80 (2019).
48. A. Kropotov, V. Kulikova, K. Nerinovski, A. Yakimov, M. Svetlova, L. Solovjeva, J. Sudnitsyna, M. E. Migaud, M. Khodorkovskiy, M. Ziegler, A. Nikiforov, Equilibrative nucleoside transporters mediate the import of nicotinamide riboside and nicotinic acid riboside into human cells. *Int. J. Mol. Sci.* **22**, 1391 (2021).
49. L. M. Henderson, C. J. Gross, Metabolism of niacin and niacinamide in perfused rat intestine. *J. Nutr.* **109**, 654–662 (1979).
50. F. Sadoogh-Abasian, D. F. Evered, Absorption of nicotinic acid and nicotinamide from rat small intestine in vitro. *Biochim. Biophys. Acta* **598**, 385–391 (1980).
51. K. Shibata, T. Fukuwatari, Organ correlation with tryptophan metabolism obtained by analyses of TDO-KO and QPRT-KO mice. *Int. J. Tryptophan Res.* **9**, 1–7 (2016).
52. F. M. Matschinsky, D. F. Wilson, The central role of glucokinase in glucose homeostasis: A perspective 50 years after demonstrating the presence of the enzyme in islets of Langerhans. *Front. Physiol.* **10**, 148 (2019).
53. M. Salas, E. Vinuela, A. Sols, Insulin-dependent synthesis of liver glucokinase in the rat. *J. Biol. Chem.* **238**, 3535–3538 (1963).
54. C. Sharma, R. Manjeshwar, S. Weinhouse, Effects of diet and insulin on glucose-adenosine triphosphate phosphotransferases of rat liver. *J. Biol. Chem.* **238**, 3840–3845 (1963).
55. A. A. Peluso, A. T. Lundgaard, P. Babaei, F. Mousovich-Neto, A. L. Rocha, M. V. Damgaard, E. G. Bak, T. Gnanasekaran, O. L. Dollerup, S. A. J. Trammell, T. S. Nielsen, T. Kern, C. B. Abild, K. Sulek, T. Ma, Z. Gerhart-Hines, M. P. Gillum, M. Arumugam, C. Ørskov, D. McCloskey, N. Jessen, M. J. Herrgård, M. A. S. Mori, J. T. Treebak, Oral supplementation of nicotinamide riboside alters intestinal microbial composition in rats and mice, but not humans. *NPJ Aging.* **9**, 7 (2023).
56. K. M. Niu, T. Bao, L. Gao, M. Ru, Y. Li, L. Jiang, C. Ye, S. Wang, X. Wu, The impacts of short-term NMN supplementation on serum metabolism, fecal microbiota, and telomere length in pre-aging phase. *Front. Nutr.* **8**, 756243 (2021).
57. V. V. Lozada-Fernández, O. deLeon, S. L. Kellogg, F. L. Saravia, M. A. Hadiono, S. N. Atkinson, J. L. Grobe, J. R. Kirby, Nicotinamide riboside-conditioned microbiota deflects high-fat diet-induced weight gain in mice. *mSystems* **7**, e0023021 (2022).
58. Z. Ren, Y. Xu, T. Li, W. Sun, Z. Tang, Y. Wang, K. Zhou, J. Li, Q. Ding, K. Liang, L. Wu, Y. Yin, Z. Sun, NAD^+ and its possible role in gut microbiota: Insights on the mechanisms by which gut microbes influence host metabolism. *Anim. Nutr.* **10**, 360–371 (2022).
59. H. A. K. Lapatto, M. Kuusela, A. Heikkinen, M. Muniandy, B. W. van der Kolk, S. Gopalakrishnan, N. Pöllänen, M. Sandvik, M. S. Schmidt, S. Heinonen, S. Saari, J. Kuula, A. Hakkarainen, J. Tampio, T. Saarinen, M. R. Taskinen, N. Lundbom, P. H. Groop, M. Tiirola, P. Katajisto, M. Lehtonen, C. Brenner, J. Kaprio, S. Pekkala, M. Ollikainen, K. H. Pietiläinen, E. Pirinen, Nicotinamide riboside improves muscle mitochondrial biogenesis, satellite cell differentiation, and gut microbiota in a twin study. *Sci. Adv.* **9**, eadd5163 (2023).
60. S. A. Trammell, M. S. Schmidt, B. J. Weidemann, P. Redpath, F. Jaksch, R. W. Dellinger, Z. Li, E. D. Abel, M. E. Migaud, C. Brenner, Nicotinamide riboside is uniquely and orally bioavailable in mice and humans. *Nat. Commun.* **7**, 12948 (2016).
61. M. V. Damgaard, T. S. Nielsen, A. L. Basse, S. Chubanava, K. Trost, T. Moritz, R. W. Dellinger, S. Larsen, J. T. Treebak, Intravenous nicotinamide riboside elevates mouse skeletal muscle NAD^+ without impacting respiratory capacity or insulin sensitivity. *iScience* **25**, 103863 (2022).
62. K. Okabe, K. Yaku, Y. Uchida, Y. Fukamizu, T. Sato, T. Sakurai, K. Tobe, T. Nakagawa, Oral administration of nicotinamide mononucleotide is safe and efficiently increases blood nicotinamide adenine dinucleotide levels in healthy subjects. *Front. Nutr.* **9**, 868640 (2022).
63. K. Yaku, K. Okabe, T. Nakagawa, Simultaneous measurement of NAD metabolome in aged mice tissue using liquid chromatography tandem-mass spectrometry. *Biomed. Chromatogr.* **32**, e4205 (2018).
64. M. V. Makarov, N. W. Harris, M. Rodrigues, M. E. Migaud, Scalable syntheses of traceable ribosylated NAD^+ precursors. *Org. Biomol. Chem.* **17**, 8716–8720 (2019).
65. R. V. Shchepin, D. A. Barskiy, D. M. Mikhaylov, E. Y. Chekmenev, Efficient synthesis of nicotinamide-1-^{15}N for ultrafast nmr hyperpolarization using parahydrogen. *Bioconjug. Chem.* **27**, 878–882 (2016).

Acknowledgments: We thank K. Hikosaka and T. Kubo for their excellent technical assistance. We also thank J. Yoshino and C. D. de Siqueira for the critical reading of the manuscript. **Funding:** This work was supported by the JSPS KAKENHI (grant nos. 20K20655 and 23K24762 to T.N. and 18K17921 and 21K11593 to K.Y.), AMED-PRIME (grant no. 24gm6710007h0003), and grants from the Kobayashi Foundation, Takeda Science Foundation, the Tamura Science & Technology Foundation, Takeda Medical Research Foundation, Takahashi Industrial and Economic Research Foundation, and Japan Foundation for Applied Enzymology to T.N., as well as grants from LOTTE Foundation, Kobayashi Foundation, Suzuken Memorial Foundation, and Novartis Foundation to K.Y. This research was also supported by Moonshot R&D (grant no. JPMJMS2021). M.E.M. and F.H. were supported in part by the National Institutes of Health, US, grant no. 1R01HL165792 and the Mitchell Cancer Institute. S.P., T.I., and M.K. were supported by the Honjo International Scholarship Foundation (no. 1190817), the Rotary Yoneyama Memorial Scholarship, and the JST SPRING (grant no. JPMJSP2145), respectively. **Author contributions:** Writing—original draft: K.Y., S.P., and T.N. Conceptualization: K.Y., S.P., T.I., A.N., and T.N. Investigation: K.Y., S.P., T.I., H.I., T.Y., H.M., and A.N. Writing—review and editing: K.Y., S.P., T.I., Y.W., S.F., H.I., T.Y., H.U., A.N., H.M., M.E.M., and T.N. Methodology: K.Y., S.P., H.M., T.I., F.H., Y.W., S.F., A.N., M.E.M., and T.N. Resources: K.Y., S.P., F.H., Y.W., S.F., H.I., T.Y., M.K., H.U., A.N., K.T., M.E.M., and T.N. Funding acquisition: K.Y., M.E.M., and T.N. Data curation: K.Y., S.P., and A.N. Validation: K.Y., S.P., A.N., M.E.M., and T.N. Formal analysis: K.Y., S.P., T.I., and A.N. Visualization: K.Y., S.P., T.I., A.N., and T.N. Project administration: A.N. and T.N. Supervision: S.P. and T.N. **Competing interests:** The authors declare that they have no competing interests. **Data and materials availability:** All data needed to evaluate the conclusions in the paper are present in the paper and/or the Supplementary Materials. The stable isotope–labeled NMN and NR can be provided by M.E.M. pending scientific review and a completed material transfer agreement. Requests for the stable isotope–labeled NMN and NR should be submitted to M.E.M. (mmigaud@southalabama.edu).

Submitted 18 June 2024
Accepted 18 February 2025
Published 21 March 2025
10.1126/sciadv.adr1538